Catalog of Nearby Isolated Galaxies in the Volume $z < 0.01$

I. D. Karachentsev,[1] D. I. Makarov,[1] V. E. Karachentseva,[2] and O. V. Melnyk[3,4]

[1] *Special Astrophysical Observatory of the Russian AS, Nizhnij Arkhyz 369167, Russia*

[2] *Main Astronomical Observatory, National Academy of Sciences, ul. Acad. Zabolotny 27, Kiev, 03680 Ukraine*

[3] *Astronomical Observatory, Taras Shevchenko University, Observatornaya 3, Kiev, 04053 Ukraine*

[4] *Institut d'Astrophysique et de Geophysique, Université de Liège, Alleé du 6 Août, 17, B5C B4000 Liege, Belgium*

(Received November 2, 2010; Revised November 25, 2010)

We present a catalog of 520 most isolated nearby galaxies with radial velocities $V_{LG} < 3500\,\mathrm{km/s}$, covering the entire sky. This population of "space orphans" makes up 4.8% among 10 900 galaxies with measured radial velocities. We describe the isolation criterion used to select our sample, called the "Local Orphan Galaxies"(LOG), and discuss their basic optical and HI properties. A half of the LOG catalog is occupied by the Sdm, Im and Ir morphological type galaxies without a bulge. The median ratio $M_{\mathrm{gas}}/M_{\mathrm{star}}$ in the LOG galaxies exceeds 1. The distribution of the catalog galaxies on the sky looks uniform with some signatures of a weak clustering on the scale of about 0.5 Mpc. The LOG galaxies are located in the regions where the mean local density of matter is approximately 50 times lower than the mean global density. We indicate a number of LOG galaxies with distorted structures, which may be the consequence of interaction of isolated galaxies with massive dark objects.

1. INTRODUCTION

The population of isolated galaxies is of great interest for testing different scenarios of the origin and evolution of galaxies. Residing in the regions of very low matter density, isolated galaxies were not subjected to a significant influence from their close neighbourhood. It is assumed that over the past several billion years the evolution of these objects was driven by purely internal reasons within the "closed box" scenario. In this sense, dynamically isolated galaxies are the reference sample to study the effects of the environment on such galaxy properties as morphology, chemical abundance and the star formation rate (SFR). A recent international conference "Galaxies in Isolation: Exploring Nature Versus Nurture" held in Granada, Spain in May 2009 illustrates of a significant interest to isolated galaxies.

According to the current data [1–3], slightly more than a half of galaxies (54%) are concentrated in the virialized groups and clusters. Another 20% of galaxies are located in the collapsing regions around the groups and clusters. Over time, the population of these regions undergoes virialization as well. The remaining quarter of galaxies are referred to as the "general field galaxies", which are distributed mainly along the diffuse filaments imbordering the cosmic voids. The standard ΛCDM model of the accelerated expansion of the universe predicts that the field population will have an increasingly weakening mutual gravitational influence, and shall hence never gather in any virialized systems.

Among the fairly common category of field galaxies one can select a sample of the most isolated galaxies based on the mutual separations to their closest neighbors. A simple and effective criterion of isolation was proposed by Karachentseva [4]. A galaxy with an angular diameter of a_1 was considered isolated if all its significant neighbors with the angular diameters of a_i in the range of

$$4 \geq a_i/a_1 \geq 1/4 \tag{1}$$

were located at the angular distances

$$X_{1i} \geq 20a_i. \tag{2}$$

At the time, in the absence of systematic data on the radial velocities and distances of galaxies, Karachentseva's criterion allowed to select in the northern sky a sample of 1 050 isolated galaxies among about 27 000 galaxies with apparent magnitudes of $m_B < 15.7^m$, which amounted to about 4% of the total. Subsequent measurements of radial velocities of the KIG galaxies [4], as well as their neighbors confirmed a good spatial isolation of these objects. Later, Karachentseva et al. [5] applied a similar criterion to search for the isolated galaxies among the extended sources of the 2MASS infrared sky survey [6]. A new 2MIG catalog covers all the northern and southern sky and contains 3 227 isolated galaxies with apparent magnitudes $K_s < 12.0^m$, and angular diameters $a_K > 30''$. The characteristic depth of the 2MIG catalog is around 6 500 km/s, and this sample contains about 6% of the galaxies with the corresponding apparent magnitudes and diameters.

For the nearby volume of space Karachentsev et al. [7] have compiled a catalog of 450 galaxies located in the sphere of a 10 Mpc radius (CNG). Most galaxies in the CNG catalog have individual distance estimates. In this most studied volume each galaxy "i" can be characterized by the tidal index

$$(TI)_i = \max\{\log(M_k/D_{ik}^3\} + C, \;\; k = 1, 2 \ldots n, \tag{3}$$

where M_k is the total mass of the neighboring galaxies, separated from the considered galaxy at the spatial distances of D_{ik}. The value of the constant C was chosen so that the condition $TI = 0$ would correspond to the case where the Keplerian period of galaxy motion relative to its main perturbing neighbor is equal to the age of the universe $T = 13.7$ Gyr. With this definition in mind, the galaxies with the positive tidal index appear to be group members, and the condition $TI < 0$ separates the population of "field galaxies". A total of 197 galaxies, or 44% made it into the latter category. If we select the most isolated objects with $TI < -2.0$, then their relative number, i.e. about 5%, turns out to be about the same as in the KIG and 2MIG catalogs. This category of very isolated nearby galaxies settles in the regions where the local matter density (conditioned by their neighbors) is two orders lower than the mean density in the CNG catalog.

Therefore, currently there are only two samples, covering the entire sky and separating about 5% of the most isolated galaxies: a small CNG sample (with $TI < -2.0$) on the scale of 10 Mpc, and a large 2MIG sample on the scale of around 90 Mpc. The latter catalog, due to the constraint on the galaxy apparent magnitude is missing a lot of dwarf systems located at large distances. There is hence a need for a new representative sample of isolated galaxies, which is limited rather by the distance of galaxies than by the apparent magnitude. We have compiled a sample of an intermediate volume, filling the gap between the CNG and 2MIG catalogs, and present it in this paper.

2. INITIAL DATA AND THE ISOLATION CRITERION

To search for isolated galaxies we used the data on radial velocities, apparent magnitudes and morphological types from the updated HyperLEDA [8] (`http://leda.univ-lyon1.fr`) and NED (`http://nedwww.ipac.caltech.edu`) databases, complemented by the measurements of radial velocities from the latest optical and HI sky surveys: SDSS, 6dF, HIPASS, and ALFALFA. The galaxies that were checked for isolation had their radial velocities relative to the centroid of the Local Group $V_{LG} < 3\,500$ km/s at the galactic latitudes $\mid b \mid > 15°$ regardless of their luminosity and morphology. Outside of this volume we as well took into account galaxies with $V_{LG} < 4\,000$ km/s and $\mid b \mid > 10°$ in order to avoid the effect of false isolation at the boundary of the sample. Each galaxy was visually examined in the DSS and SDSS images to exclude the cases of confusion in the coordinates, error identifications, and questionable radial velocities, which often arise in the implementation of automated sky surveys. In addition, we performed a morphological classification of galaxies and estimated their apparent magnitudes if they were absent in the NED and HyperLEDA

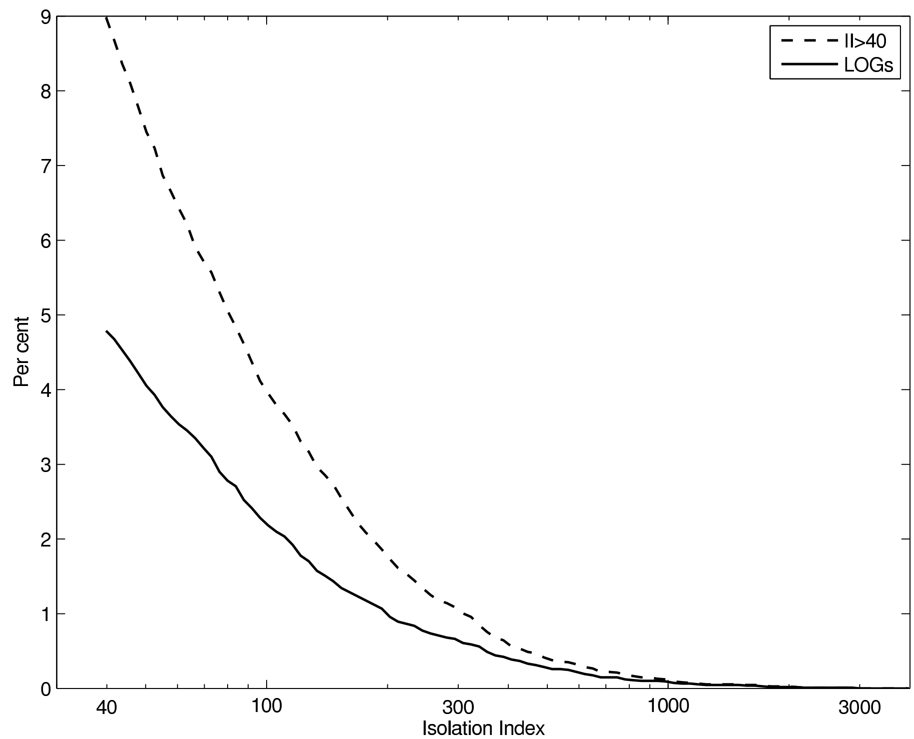

Figure 1. The relative number of galaxies as a function of the isolation index II among 10 900 galaxies with $V_{LG} < 3500$ km/s (the dashed line). The solid line describes a similar dependence for the LOG catalog.

databases. We used apparent magnitudes of galaxies in the K_s photometric band from the 2MASS survey [6] as a basis. Apparent magnitudes in other bands (B, V, R, I, J, H) were transformed into the K-band taking into account the average color indices for each morphological type [9, 10].

A total of 10 900 galaxies were checked in the above volume for galaxy system membership. Each galaxy was attributed the total mass M, proportional to its K-luminosity

$$M/L_K = \kappa M_\odot/L_\odot, \tag{4}$$

where κ is a dimensionless value. A remarkable property of the K-luminosity is its low sensitivity to the internal absorption in a galaxy, as well as to the presence of a young blue stellar population. At $\kappa = 1$ the K-band luminosity corresponds to the stellar mass of a galaxy. To estimate the total mass of a galaxy we have adopted the value $\kappa = 6$, at which the structure and the known virial mass of the nearby groups is best reproduced.

Pairwise combining the galaxies into systems, we assumed that each virtual pair "ik" has to satisfy the condition of negative total energy

$$V_{ik}^2 R_{ik}/2GM_{ik} < 1, \tag{5}$$

and the condition of its components location within the "sphere of zero-velocity" that separates the given pair against the global Hubble expansion

$$\pi H_0^2 R_{ik}^3 / 8 G M_{ik} < 1. \tag{6}$$

Here V_{ik} and R_{ik} denote the radial velocity differences and the projected separations of the virtual pair components, M_{ik} is their total mass, expressed in terms of the K-luminosity at $\kappa = 6$, while G and H_0 are the gravitational constant and the Hubble parameter, respectively. The clustering algorithm involves a sequential review of all the galaxies of the original sample and the subsequent union of bound pairs with common members into groups/clusters of galaxies.

Having applied this algorithm that takes into account individual characteristics of galaxies, about 54% of all the galaxies were combined into systems of different populations. Among the remaining population of field galaxies we then selected especially isolated ones, satisfying a higher value of the κ parameter. To this end, we used the condition

$$\kappa = 6 \times (II), \tag{7}$$

where the dimensionless value (II) has a sense of the "isolation index." At $(II) = 40$ the total of about 10% of galaxies retain their isolation. This sample of 990 galaxies formed the basis of our catalog.

The isolation criterion (5–7) is actually based on the condition of dynamical isolation of a galaxy in the 3D-space, rather than in the sky. Therefore it has a clearer physical meaning than the 2D Karachentseva's criterion (1–2). However, not all the galaxies in the volume have their radial velocities measured. To exclude the cases where the galaxy, isolated according to (5–7) may reveal a nearby neighbor in the sky with a velocity close to the velocity of the considered galaxy itself, we additionally used Karachentseva's constraint (1–2) to the already selected 990 galaxies. A consecutive use of two criteria (5–7) and (1–2) reduced our sample from 990 to 520 galaxies.

Clearly, not all the galaxies, excluded by the additional criterion (1–2) would appear to be not isolated when their "significant" neighbors in the projection would eventually have their radial velocities measured. Moreover, the results of our pilot program measuring the radial velocities of galaxies in the vicinity of the isolated galaxy candidates have shown [11] that about 80% of them retain their isolation (most of the "significant" neighbors turn out to be the distant background galaxies with a typical velocity difference of $\Delta V_{ik} > 10\,000$ km/s). Despite this, we prefer to use the more rigorously selected sample, satisfying both the (5–7) and (1–2) criteria for the further analysis.

In Fig.1, the upper (dashed) curve shows how the relative number of galaxies that satisfy the (5–6) criterion decreases with an increasing value of the isolation index II. For example, going from $II = 40$ to $II = 400$ the percentage of isolated galaxies drops by an order. The solid (lower) line corresponds to the case when an additional constraint is applied to the sample using the condition (1–2). At $II = 40$ the sample of isolated galaxies numbers 520, i.e., approximately the same relative number (about 5%) as in the KIG and 2MIG catalogs. We have designated the sample of these 520 galaxies as the "Local Orphan Galaxies" (LOG) and shall adhere to this acronym further down.

An example of a situation where new redshift measurements can break the isolation of the galaxy, selected by the (5–7) criterion, is LOG 227. Near the galaxy KUG 0956+420 with velocity $V_h = 1\ 682$ km/s there was discovered a neighboring galaxy KUG 0956+419, the radial velocity of which $V_h = 1\ 737$ km/s was measured with a great error (± 340 km/s). Both blue dwarf galaxies may be forming a physical pair with a projection distance of 40 kpc.

3. THE LOG CATALOG

A list of 520 "orphan"galaxies in the Local Supercluster and its surroundings is presented in Table 1. Its columns contain the following data: (1) is the running number in the catalog, (2) is the name or the number of a given galaxy in the known catalogs as they are fixed in the HyperLEDA and NED databases; in some cases the long names of galaxies from the past surveys (SDSS, 6dF, HIPASS) are listed with an ellipsis and with no coordinate part, (3)—equatorial coordinates for epoch (2000.0), (4)—radial velocity of the galaxy relative to the centroid of the Local group and its measurement error (in km/s), (5)—morphological type of the galaxy in the digital de Vaucouleurs scale [12], (6)—integrated apparent magnitude of the galaxy in the K_s-band, adopted from the 2MASS survey or converted from other photometric bands taking into account the morphological type; in the latter case, which dominates, the K magnitude error may reach about 0.5^m; (7)—the value of the isolation index in the condition $M/L_K = 6 \times (II) \times (M_\odot/L_\odot)$, at which the galaxy still retains its isolation, (8)—the logarithm of the flux in the HI 21 cm line (in Jansky/km/s) according to the HyperLEDA; in some cases (marked by a colon), the upper limit of the HI-flux was estimated according to the HIPASS survey data or other available sources, (9)—in this column "+" marks the galaxies satisfying Karachentseva's criterion [4] with a significant margin, (10)—the comment column contains a brief reference to the following data: "IR" indicates the presence in a galaxy of an infrared flux in the IRAS survey, "F" marks the belonging of a galaxy to the flat systems from the RFGC and 2MFGC catalogs, "pec" marks the presence of a peculiar structure, "Mrk" indicates the belonging of a galaxy to the list of Markarian active objects, and "KIG"—to the isolated galaxies from the KIG catalog.

4. BASIC CHARACTERISTICS OF LOG GALAXIES

Figure 2 presents a distribution of isolated galaxies in the radial velocity intervals of 250 km/s. The unshaded histogram shows the total number of galaxies satisfying the $II > 40$ criterion, and the shaded part corresponds to the LOG catalog galaxies, for which the additional isolation condition (1–2) is applied. The diamonds mark the percentage of LOG galaxies to the total number of galaxies in each velocity interval (the right-hand scale). As we can see, the relative number of isolated galaxies is practically independent of the distance, undergoing the statistical fluctuations around the mean value of 4.8%. An approximate constancy of the LOG galaxy percentage indicates that the isolation criterion we used works equally effectively both in the nearby and distant volumes. This circumstance is not trivial. For example, in a sample of isolated galaxies from the SDSS survey [13] their relative number varies with distance more than tenfold.

The overall distribution of 520 LOG galaxies in the sky in equatorial coordinates is demonstrated in Figure 3. The galaxies from the closer volume with $V_{LG} < 2000$ km/s are marked by the circles of a larger diameter. The region of a significant galactic absorption along the Milky Way is shown by the ragged gray stripe. The distribution of isolated galaxies outside the region $\mid b \mid < 15°$ looks pretty uniform. Some deficiency of isolated objects is noticeable in the direction of the known nearby clusters Virgo, Fornax and similar groups around M81 and CenA.

An important characteristic of each galaxy sample is its morphological composition, which retains the features of the evolution of galaxies. Figure 4 shows the distribution of 520 LOG galaxies, as well as all the 990 isolated galaxies with $II > 40$ according to the morphological type. As follows from this histogram, the use of an additional isolation condition (1–2) does not introduce any special selectivity according to the morphological type. The latest types of galaxies T = 8–10, i.e. Sdm, Im, Ir are the most common members of the LOG sample. They account for 51% of all galaxies.

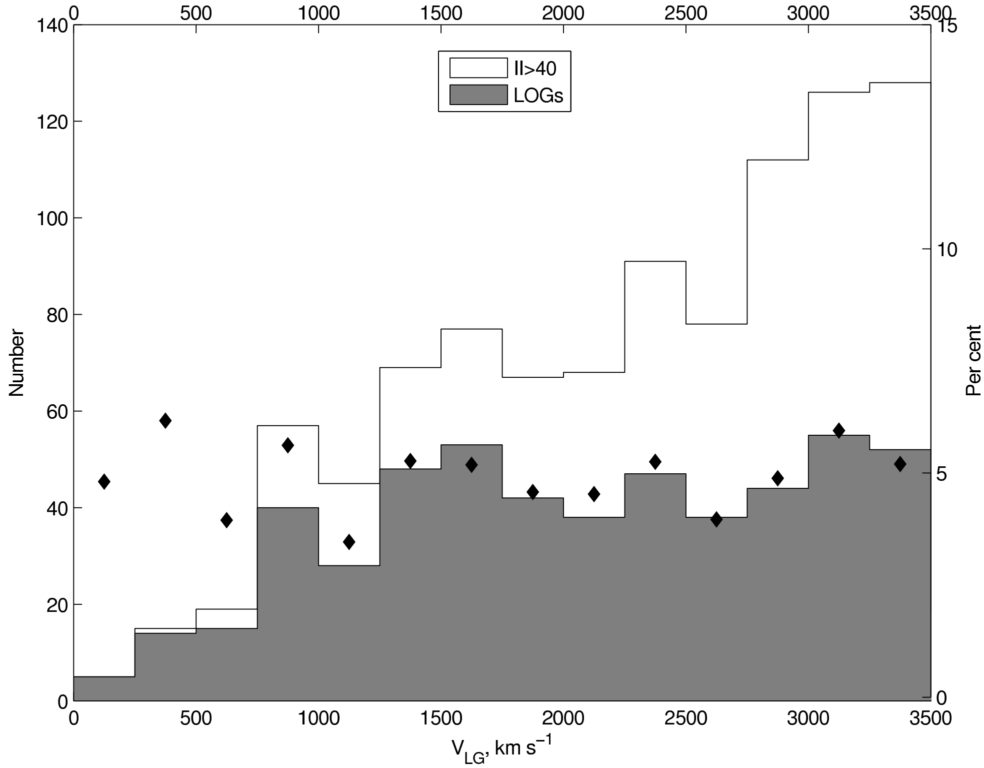

Figure 2. The distribution of galaxies with the $II > 40$ isolation index (the unshaded histogram) and LOG galaxies (the gray histogram) by radial velocity. The diamonds indicate the relative number of LOG galaxies in each velocity interval (percentage of the total number N = 10 900, the right-hand scale).

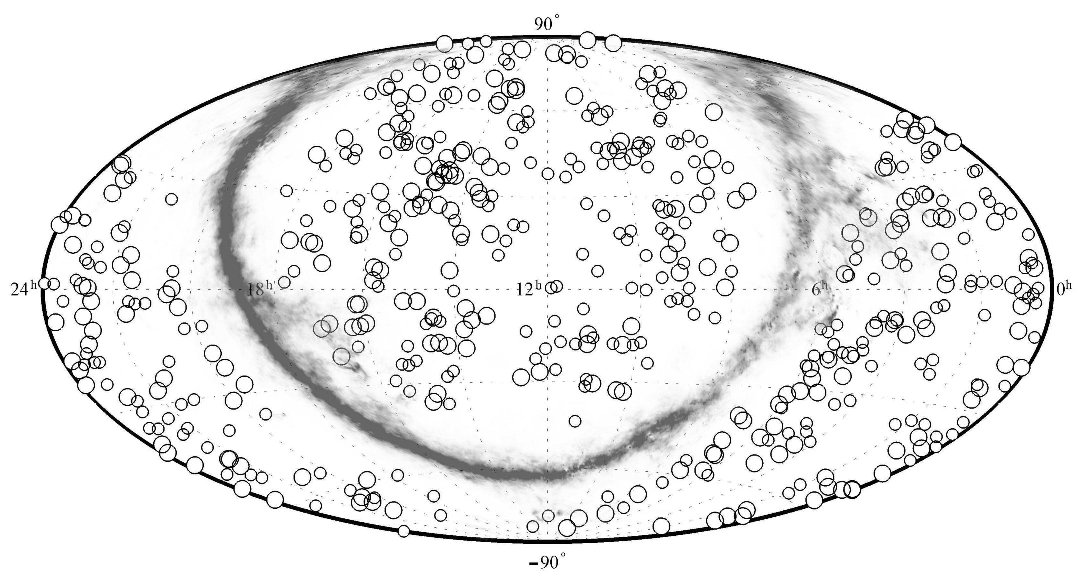

Figure 3. The distribution of 520 LOG galaxies on the sky in equatorial coordinates. The galaxies with radial velocities $V_{LG} \leq 2\ 000$ km/s are marked by larger circles.

Table 1. Catalog of isolated galaxies in the Local Supercluster and its neighborhood

LOG	Name	RA (J2000.0) Dec.	V_{LG}	$\pm$	T	K_s	lg II	lg F_{HI}	K73	Note
(1)	(2)	(3)	(4)		(5)	(6)	(7)	(8)	(9)	(10)
1	ESO149-013	000246.3−524618	1363	80	10	13.39	1.78	1.06	+	
2	ESO149-018	000714.5−523712	1744	9	9	13.61	1.86	0.74	+	
3	UGC00064	000744.0+405232	554	17	10	12.80	1.97	1.24	+	
4	UGC00063	000750.8+355759	715	5	10	12.72	2.03	0.36	+	
5	ESO538-024	001017.8−181551	1634	5	10	13.20	1.87	0.84	+	
6	PGC130903	001108.7−385915	3180	43	6	13.95	2.17	0.3 :		
7	6dF...	001408.3−353648	3268	29	9	14.31	2.25	0.71	+	
8	SDSS...	001500.1−110804	3467	5	6	14.78	1.92	0.3 :	+	
9	ESO241-027	001502.7−431731	3235	74	6	12.44	1.99	0.05	+	
10	6dF...	001550.9−225511	3213	34	6	12.54	2.07	0.56	+	
11	ESO194-002	001830.4−473921	1433	10	9	13.92	1.69	0.3 :	+	
12	AM0016-575	001909.3−573830	1636	5	2	12.12	1.87	1.28	+	pec
13	UGC00199	002051.8+125122	2015	5	10	14.64	1.72	0.53	+	
14	ESO150-005	002225.6−533851	1344	5	8	11.32	2.02	1.11	+	
15	NGC0101	002354.6−323210	3411	30	6	10.19	2.01	1.12	+	IR
16	UM240	002507.4+001846	3397	13	9	15.64	2.30	0.3 :	+	
17	6dF...	002755.3−031101	3372	10	6	11.79	2.05	0.46	+	
18	UM040	002826.6+050016	1523	5	2	13.26	1.96	0.70	+	
19	UGC00285	002851.1+285622	2428	11	2	11.60	2.08	0.04	+	IR
20	UGC00288	002903.6+432554	463	5	10	13.32	1.85	0.71	+	
21	UGC00313	003126.1+061224	2237	35	4	11.33	2.12	−0.09	+	IR
22	HS0029+1748	003203.1+180446	2410	30	9	15.12	2.53	0.3 :		
23	ESO294-020	003209.7−401605	1393	11	8	11.13	1.90	0.44	+	IR
24	UGC00328	003322.1−010717	2139	5	8	12.78	1.97	1.11	+	
25	CGCG409-040	003448.9+072701	739	10	2	11.44	1.76	−0.58	+	
26	CGCG500-052	003707.6+284954	2233	16	9	12.42	2.08	0.64		F
27	PGC002235	003726.1−370311	3400	24	6	14.07	2.37	0.3 :		
28	HIPASSJ0041-01b	004139.6−020042	2096	9	10	13.49	2.01	0.52	+	
29	ESO540-016	004214.7−180942	1623	5	6	12.50	1.67	1.52	+	IR,F
30	Andromeda IV	004230.1+403433	522	9	10	13.98	1.77	1.36	+	
31	CGCG410-002	004448.4+050809	3066	21	0	11.66	1.94	0.3 :	+	IR
32	UGC00477	004613.1+192924	2870	10	7	11.81	2.11	1.59		F
33	UGCA014	004747.5−095358	1450	5	7	11.93	2.00	1.40		F
34	ESO079-007	005003.8−663312	1511	11	7	11.67	2.00	0.84		IR
35	PGC169954	005154.6+232851	2847	8	9	13.90	1.88	0.01		
36	ARK018	005159.6−002912	1764	8	1	12.58	1.89	1.17		
37	MCG-01-03-027	005217.2−035760	1520	28	6	13.93	1.85	1.05	+	
38	ESO411-027	005251.7−271933	1852	10	8	13.43	1.95	0.27		
39	IC1596	005442.8+213122	2891	5	3	11.41	1.61	0.70	+	IR,KIG
40	UGC00578	005621.1+394933	1728	31	4	11.46	2.32			IR
41	ESO474-045	005721.3−242219	1894	5	8	13.73	2.03	0.64	+	
42	UGC00614	005936.2+353337	2591	13	6	11.98	2.74	0.67	+	IR
43	ESO151-019	010220.8−541923	1261	9	8	11.81	2.15	0.86	+	
44	UGC00655	010401.2+415035	1084	5	8	12.57	1.63	1.21	+	
45	MCG-04-03-052	010632.4−234045	3500	33	5	13.25	2.06	0.54	+	
46	UGC00685	010722.4+164104	351	5	9	12.00	2.24	1.06	+	KIG
47	NGC0406	010725.1−695245	1335	5	5	10.17	1.63	1.53	+	IR
48	UGC00695	010746.4+010349	764	5	9	12.76	2.21	0.53		
49	KK11	010821.9−381234	605	10	9	14.26	2.05	0.67	+	
50	NGC0404	010927.0+354304	218	24	−3	8.55	1.78	1.59	+	IR
51	ESO243-050	011048.8−422231	1423	8	10	12.12	2.03	0.84	+	
52	AM0117-681	011901.8−680244	1883	9	7	12.69	2.13	0.72	+	
53	LSBGF352-021	012658.6−350542	2068	9	10	15.26	1.98	0.16		
54	AM0126-653	012822.4−651615	1461	22	5	11.55	1.91	0.95	+	IR
55	UGC01054	012848.3+342047	2889	5	7	14.25	2.60	0.86		F
56	FGC0175	013531.5+020154	2731	5	8	13.65	1.92	0.65	+	F
57	NGC0620	013659.7+421924	2708	19	7	10.99	1.94	2.00	+	IR

(1)	(2)	(3)	(4)		(5)	(6)	(7)	(8)	(9)	(10)
58	UGCA020	014314.7+195832	677	5	10	13.61	1.75	0.97	+	pec
59	ESO114-007	014630.4−584027	2063	9	8	11.98	2.14	1.22	+	
60	UGC01207	014726.3+820934	1500	5	8	14.01	1.65	0.75		
61	NGC0685	014742.8−524543	1234	16	5	9.18	1.62	1.54	+	IR
62	UGC01198	014917.7+851538	1408	38	−2	10.89	1.81	0.02	+	IR
63	KUG0148-067	015128.4−063060	2205	5	7	12.40	1.93	1.03	+	
64	ESO354-021	015833.3−345147	3046	43	4	13.12	1.79	0.54	+	IR
65	UGC01464	015907.6+015324	3049	75	8	14.01	2.29	0.3 :	+	
66	ESO153-019	020539.2−560411	2014	30	6	12.47	1.96	0.32	+	
67	ESO030-008	020901.7−755606	1054	60	7	12.46	1.88	1.39	+	F
68	PGC138508	021223.2+131227	2375	27	8	13.80	2.41	0.00		
69	PGC169963	021336.1+231528	2617	8	8	14.78	2.71	−0.05		
70	UGC01756	021653.9+021212	3098	6	2	11.67	1.98	0.3 :	+	IR
71	KUG0215+005	021808.1+004530	2820	5	8	14.72	1.88	0.3 :	+	
72	ESO355-005	021839.7−363152	2399	30	8	14.68	1.64	0.57		
73	NGC0918	022550.8+182946	1648	5	5	8.93	2.08	1.22	+	IR,KIG
74	UGC01970	022954.0+251523	2073	5	6	11.14	1.71	1.02	+	F
75	UGC01975	023014.7+330757	3369	14	5	11.95	1.88	0.48	+	F,KIG
76	UGC01999	023152.6+190911	1110	5	5	12.92	2.03	1.32	+	F
77	UGC02082	023616.1+252526	862	6	6	9.97	1.82	1.66		IR,F,KIG
78	ESO479-020	023908.2−223944	2999	11	5	12.30	1.84	0.99	+	
79	UGC02143	023936.6+360452	2930	9	2	11.27	1.83	0.64		IR
80	ESO546-021	024742.8−185025	3037	5	7	13.87	1.66	0.54		F
81	CGCG463-025	025019.7+190643	1362	5	9	12.27	2.67	0.47		
82	UGC02352	025205.4+042215	1872	8	7	14.40	2.58	0.68	+	F
83	UGC02392	025546.4+334560	1712	5	5	13.22	2.39	0.78	+	
84	UGC02429	025709.2+011935	1822	6	7	12.88	2.19	0.84	+	
85	UGC02432	025726.8+100812	840	5	10	13.84	2.57	0.85	+	
86	UGCA047	025824.3−041744	2397	10	6	11.37	1.61	0.85	+	IR
87	NGC1156	025942.2+251414	507	5	9	9.46	2.12	1.67	+	IR,KIG
88	KKH018	030305.8+334140	375	5	10	13.49	1.76	0.40	+	
89	ESO547-004	030330.6−201034	3275	10	5	13.29	1.99	0.64	+	
90	MCG-01-09-010	030931.2−045444	3136	5	6	11.29	1.96	0.77		
91	MCG+04-08-013	031419.8+240914	1421	9	6	13.44	2.61	1.05		
92	KDG032	031856.7−103247	1910	9	10	14.02	1.61	0.84	+	
93	NGC1337	032806.0−082319	1216	7	6	9.19	1.87	1.80	+	IR
94	UGC02809	033933.2+194703	1368	6	8	12.59	1.60	0.77	+	
95	HIPASSJ0341+18	034201.8+180830	1369	9	8	12.89	1.60	0.48		
96	2MASX...	034559.4−123149	900	25	1	11.17	2.28	0.3 :	+	IR
97	UGC02899	035424.6+063524	3482	5	5	12.14	2.11	1.01	+	F
98	UGC02905	035700.1+163121	345	5	10	13.60	2.19	0.66		
99	HIPASSJ0358+10	035824.2+095845	2003	9	8	13.70	2.82	0.84	+	
100	MCG-01-11-002	040615.9−083809	2777	5	8	13.72	1.75	0.74	+	pec
101	PGC103224	040755.9−444750	3380	31	7	14.73	2.38	0.15	+	
102	[KKS2000]53	040904.1−083737	834	5	9	12.51	2.08	0.77		
103	2MASX...	041202.3−101841	2815	74	4	12.70	2.60	0.3 :		IR
104	ESO420-013	041349.7−320025	3449	36	−1	9.47	1.79	0.3 :	+	IR
105	UGC02997	041604.9+081049	1590	19	2	10.19	2.05	−0.03	+	IR
106	6dF...	041804.5−214740	3468	74	6	13.52	2.55	0.3 :	+	
107	UGC03045	042641.7+202428	1429	5	5	9.58	2.48	0.3 :		F
108	HIPASSJ0426-07	042647.9−073332	2368	9	8	14.76	1.92	0.64	+	
109	UGC03053	042809.7+213919	2452	5	6	9.71	2.24	0.75	+	IR
110	ESO251-003	042841.3−461916	1194	9	9	13.90	1.72	0.57		
111	ESO202-035	043216.4−494033	1663	18	5	10.03	1.90	1.58	+	IR,F
112	2MASX...	043342.0−333046	2677	64	1	11.03	2.54	0.3 :		
113	ESO304-002	043519.8−421212	2030	51	2	11.84	2.35	0.3 :	+	IR
114	MCG-02-12-046	043624.6−093049	2327	7	8	12.70	1.84	1.13	+	IR,pec
115	PGC971141	043632.5−110009	1727	17	8	13.78	2.25	0.3 :	+	
116	ESO551-030	044226.8−172713	3067	30	7	12.39	1.83	0.75	+	
117	KKH028	044344.0+025954	3463	5	10	13.49	2.36	0.55	+	
118	APMUKS...	044720.7−151518	2375	49	10	14.55	1.92	0.31		

(1)	(2)	(3)	(4)		(5)	(6)	(7)	(8)	(9)	(10)
119	LSBGF304-013	045010.5−394745	2052	22	10	12.27	2.03	0.66	+	
120	ESO552-016	045228.5−191734	2918	5	8	11.45	2.32	0.58		F
121	DDO229	045253.0−251445	1214	9	8	11.11	1.85	1.40	+	IR
122	NGC1705	045413.5−532140	401	29	9	10.52	2.20	1.18	+	IR
123	ESO552-031	045803.2−190727	1527	5	7	13.67	1.81	0.46	+	
124	CGCG445-001	045902.7+122403	3412	5	2	11.24	2.66	0.36		IR
125	ESO252-007	050301.3−431756	2742	74	4	11.72	2.53	0.47	+	IR
126	DDO35	050324.6+162416	1396	5	8	10.82	2.57	1.25	+	IR
127	UGC03247	050638.5+084033	3328	7	4	11.98	2.16	0.77	+	
128	ESO553-016	051105.9−182537	3415	5	8	13.36	2.05	1.01		
129	ESO423-002	051516.3−303135	1285	7	6	10.28	1.85	1.25	+	IR,F
130	UGC03288	051930.9+040746	2983	9	8	13.89	3.02	0.60		
131	MCG+12-06-004	052426.4+711134	3467	10	6	12.88	2.39	0.24		
132	ESO253-002	052436.2−460241	3366	9	8	13.03	1.70	0.62	+	
133	UGC03303	052459.5+043018	446	5	8	13.09	2.10	1.44	+	
134	ESO553-046	052705.7−204041	372	10	9	12.19	2.47	0.43	+	IR
135	MCG-03-14-017	052814.1−160728	2017	5	6	11.15	1.73	1.13	+	IR
136	ESO554-002	052907.6−195602	2756	39	6	12.47	1.64	0.78	+	IR
137	MCG-02-15-001	053139.9−102332	2535	36	4	10.08	1.90	0.41	+	IR,F
138	ESO487-030	053718.7−262552	1290	8	7	10.94	1.85	1.11	+	
139	ESO306-013	053858.3−414414	788	75	9	11.04	1.67	0.65	+	IR
140	[KKS2000]54	054155.2−123336	2090	13	10	11.94	1.73	0.55	+	
141	IC2147	054328.1−302942	1093	5	7	10.76	1.92	1.20	+	IR
142	ESO253-019	054401.9−453017	821	75	10	14.58	2.21	0.3 :		
143	ESO488-017	054729.0−233434	837	11	4	11.67	2.43	0.63	+	IR
144	ESO555-002	055026.7−194333	2191	7	4	10.00	1.66	1.34	+	IR,F
145	ESO120-016	055135.3−590244	3415	10	3	9.81	2.18	0.98	+	IR,F
146	2MASX...	055302.3−114420	3039	8	3	11.68	2.52	0.88	+	IR
147	HIPASSJ0554-35	055354.2−355729	2720	9	9	13.75	1.60	0.62	+	
148	ESO488-044	055550.8−224825	3104	10	4	13.37	1.83	0.56	+	
149	ESO425-001	060010.3−314714	1128	9	9	12.02	1.71	0.99		
150	RFGC1042	060143.4−345642	1065	10	8	14.41	2.12	0.76		F
151	UGC03394	060449.6+560957	1945	5	7	12.55	2.24	0.78	+	
152	UGC03403	061032.9+712245	1444	5	5	9.96	1.67	1.03	+	IR,F
153	UGC03409	061052.6+643403	1516	5	10	14.19	2.01	1.01	+	
154	ESO121-020	061554.2−574332	307	5	10	13.75	2.04	0.90		
155	ESO206-016	063109.7−522507	918	5	10	13.41	1.98	0.76	+	
156	UGC03485	063456.3+655008	1438	7	7	14.80	1.91			F
157	ESO206-017	063819.6−515710	753	10	6	13.55	1.67	0.68	+	F
158	ESO308-022	063932.7−404315	557	5	10	13.27	2.10	0.51	+	
159	[HS98] 011	064332.3+634226	3042	15	10	14.37	2.17	0.38		
160	ESO255-019	064548.2−473152	785	5	8	11.59	1.72	1.27	+	
161	ESO309-005	065302.9−391613	1634	10	3	11.19	2.25	0.81	+	IR
162	ARGO	070518.8−583113	279	9	8	11.33	1.90	1.54	+	
163	UGC03672	070627.6+301919	964	9	10	13.74	2.10	1.48		pec
164	ESO088-004	071006.5−631544	2037	52	1	10.85	1.70	0.3 :	+	IR
165	ESO035-001	071042.4−733037	2819	28	4	10.47	2.34	0.47	+	IR
166	UGC03761	071504.3+380843	3359	5	7	12.71	2.18	0.58	+	F
167	ESO162-015	071523.7−550435	2537	10	5	12.45	1.87	0.89		
168	UGC03748	071527.3+652629	2620	12	7	13.61	2.12	0.88	+	
169	CGCG309-028	071804.4+682034	2796	27	0	10.87	2.12		+	
170	UGC03826	072427.9+614138	1854	5	7	13.00	1.84	1.42	+	IR,KIG
171	UGC03845	072642.7+470538	3083	5	4	10.72	1.87	0.71		IR
172	UGC03876	072917.5+275358	811	5	6	12.89	2.00	1.06	+	IR,F,KIG
173	SDSS...	073058.9+410960	892	5	9	13.76	1.89		+	
174	ESO059-001	073118.2−681117	246	9	8	11.20	1.68	1.24	+	
175	ESO035-012	074001.1−762619	1190	9	10	12.44	1.71	0.72	+	
176	KUG0738+493	074232.4+491130	3015	14	7	11.96	1.97		+	
177	UGC04115	075701.8+142327	213	5	10	12.16	1.78	1.19	+	
178	UGC04117	075726.0+355621	756	5	8	12.40	1.82	0.68	+	
179	NGC2504	075952.3+053630	2419	75	4	11.42	2.29	0.76	+	IR,pec

(1)	(2)	(3)	(4)		(5)	(6)	(7)	(8)	(9)	(10)
180	UGC04176	080242.8+404043	3092	41	7	12.65	2.29	0.70	+	pec
181	UGC04204	080524.9+555700	3063	8	8	14.17	2.32	0.43	+	
182	CGCG148-111	080547.7+301401	2295	36	6	13.16	2.45		+	F
183	UGC04247	080903.6+164039	2717	8	7	12.93	2.60	1.22		F
184	UGC04254	080924.0+003634	1610	5	5	10.62	1.87	0.75	+	IR
185	UGC04258	081047.8+465444	3172	8	6	12.08	1.62	0.67	+	F
186	UGC04267	081256.4+545808	2694	75	6	11.73	2.26		+	IR
187	UGC04307	081801.4+475109	3164	5	6	12.46	1.62			
188	NGC2574	082048.2−085506	2635	5	4	9.79	1.67	0.95		
189	SDSS...	082712.8+265127	1779	5	9	14.86	2.06		+	
190	CGCG032-035	083121.6+070000	1702	34	8	12.85	1.72		+	
191	UGC04537	084244.9+354528	2883	5	6	13.49	2.53	0.70	+	F
192	MCG-01-23-002	084900.4−074947	2667	7	4	10.55	2.30	0.65	+	IR,F
193	ESO060-015	085003.7−700736	3284	10	5	11.45	1.75	0.77	+	IR,F
194	LSBCD563-06	085222.8+210050	3456	5	10	15.32	1.66	0.3 :	+	
195	UGC04684	085640.7+002230	2316	7	7	12.23	2.00	0.85	+	IR,KIG
196	NGC2722	085846.2−034236	2535	8	3	10.41	1.73	0.86	+	IR
197	UGC04722	090023.5+253641	1705	7	7	12.14	2.15	1.29	+	IR,F,pec,KIG
198	KUG0857+479	090058.5+474743	3175	48	4	11.19	1.63		+	
199	NGC2731	090208.4+081806	2385	23	6	10.47	2.07	0.42	+	IR
200	UGC04711	090322.8+784505	3480	40	3	12.69	1.93		+	
201	KKH46	090836.5+051727	409	5	10	15.71	1.68	0.42		
202	LSBC D634-03	090853.5+143455	181	12	10	14.98	1.69	−0.60	+	
203	CGCG121-027	090934.4+251323	2200	37	9	12.75	2.34	0.3 :	+	
204	ESO006-005	090947.4−833130	1771	20	7	13.87	1.61	0.59	+	
205	ESO018-015	091011.5−791404	1431	10	6	11.78	1.65	1.07	+	IR
206	CGCG006-011	091125.3−025257	3371	10	5	13.03	1.71	0.60	+	IR
207	SDSS...	091126.7+455226	3415	20	6	13.77	1.99		+	
208	IC2450	091705.3+252545	1607	32	3	10.92	1.90	0.3 :		IR,Mrk
209	UGC04925	091819.8+174512	2881	5	7	12.18	2.00	1.02	+	F
210	UGC04922	091836.5+475221	2022	5	8	11.23	1.70	1.36	+	
211	FGC0878	092050.4−034659	3262	12	8	14.49	2.17	0.3 :	+	F
212	CGCG062-024	092059.6+110333	1128	15	9	12.99	1.78	0.3 :		
213	KUG0917+461	092110.8+455316	1884	41	4	11.58	1.70		+	IR,KIG
214	UGC04970	092145.6+393129	2417	47	5	12.03	2.03	0.58	+	F
215	CGCG151-073	092310.9+264905	2375	7	9	13.23	1.68	0.48	+	
216	UGC05023	092601.2+192301	2404	10	9	11.73	2.26	0.37		IR,Mrk
217	UGC05078	093145.8+034343	3021	8	7	13.58	1.93	1.18	+	F
218	UGC05135	093836.2+431037	1717	67	6	13.17	2.14			
219	UGC05114	094003.2+820617	1811	11	9	13.27	1.84	0.49	+	pec
220	6dF...	094208.4−233544	3043	74	0	11.05	1.66	0.3 :	+	
221	SBS0945+594	094841.6+591539	2313	5	4	11.87	1.86		+	IR,Mrk
222	MRK1426	094918.4+483350	1906	26	4	13.67	2.14	0.19		Mrk
223	SDSS...	095058.8+104805	3017	5	5	13.24	1.81	1.00		
224	UGC05299	095241.3−001103	2705	8	8	12.99	1.98	0.78	+	
225	6dF...	095536.6−165756	2759	74	8	12.72	1.92	0.3 :		
226	UGC05309	095711.4+804435	3252	8	8	14.41	1.98	0.52		
227	KUG0956+420[1]	095930.0+414601	1678	36	9	14.54	2.13			
228	KUG0956+457	100005.2+453111	1708	5	9	14.60	1.81			
229	ESO567-012	100526.0−174757	2780	75	4	11.05	1.64	0.3 :	+	
230	KUG1003+466	100646.7+462304	2417	38	7	14.37	1.96			
231	UGC05467	100812.9+184225	2768	26	−2	10.83	2.10	0.64	+	IR
232	HIPASSJ1008-33	100828.7−330837	1337	9	10	14.30	1.81	0.50		
233	SBS1006+578	100935.4+573401	1593	5	9	14.33	1.70	0.51	+	Mrk
234	NGC3139	101005.2−114642	1157	10	1	10.25	1.98	0.3 :		
235	UGC05493	101117.9+002633	3436	5	5	11.08	2.30	0.78	+	IR
236	UGC05526	101428.6+155411	2928	40	5	12.72	1.72	0.3 :		

[1] Probably this galaxy makes a pair with KUG0956+419 having $V_{LG} = 1733$ km/s

(1)	(2)	(3)	(4)	(5)	(6)	(7)	(8)	(9)	(10)
237	SDSS...	101456.7+604557	3331 95	8	13.44	1.99		+	
238	UGCA208	101628.2+451918	1671 5	9	12.65	1.88	0.65		Mrk
239	IC2563	101851.9−323548	1044 5	7	12.64	1.88	0.54	+	
240	ESO567-048	101941.6−174460	631 5	8	10.28	1.90	1.11		
241	MRK0630	102310.4+175746	3425 45	9	11.67	1.93	0.5 :		IR,Mrk
242	KUG1028+412	103118.4+410226	2568 5	9	15.23	2.12			
243	PGC031148	103238.2−172534	2377 5	8	13.09	1.78	0.64	+	pec
244	MRK1434	103410.1+580349	2247 75	9	15.24	1.62			Mrk
245	UGC05744	103504.8+463341	3365 30	1	11.04	1.74			IR,Mrk
246	UGC05825	104211.1+234448	3390 8	4	10.78	2.15	0.90	+	
247	DDO87	104936.5+653150	467 5	10	12.83	1.76	1.21		
248	CGCG038-048	105512.6+055145	3320 18	3	12.41	2.05	0.5 :	+	
249	ESO437-071	105519.3−302804	1875 5	6	10.90	1.71	1.00	+	
250	MCG-02-28-031	105938.2−153135	2785 6	6	11.45	2.12	1.01	+	F
251	UGC06138	110439.7+274326	2506 5	5	11.00	1.83	0.94		
252	2MASX...	110443.6−290633	2103 74	6	12.49	1.76	0.5 :	+	F
253	ESO438-002	110542.0−312737	3426 5	6	13.25	2.00	0.5 :	+	F
254	KKSG23	110611.5−142432	789 5	10	13.22	1.61	1.04	+	
255	2MASX...	110703.8−173622	749 29	8	13.09	1.69	0.74		
256	CGCG364-019	110734.3+825114	1876 26	0	13.06	1.96		+	
257	KUG1107+403	111025.2+400311	2932 29	6	13.42	1.89		+	
258	PGC034171	111329.0−061525	2312 5	6	11.17	1.77	0.29		
259	KK100	111359.3+111944	2822 5	7	14.68	1.70	0.3 :	+	
260	ESO265-018	111436.1−431610	2608 39	10	13.66	1.80	0.65		pec
261	UGC06383	112202.6+424909	3177 8	6	13.46	2.12	0.72		IR,F,KIG
262	MCG-03-29-006	112232.9−173412	3399 42	4	13.12	1.68	0.3 :	+	IR
263	UGC06517	113202.4+364153	2472 9	4	11.10	1.85	0.82	+	IR
264	2MASX...	114234.8−165210	2226 40	−3	10.90	1.62	0.5 :		
265	SDSS...	114805.4+005929	2867 66	8	14.93	1.69	0.5 :		
266	ESO504-016	114834.4−255710	2890 34	1	12.46	1.72	0.3 :	+	
267	6dF...	115042.6−101312	2131 42	8	12.74	1.63	0.43	+	
268	UGC06890	115511.7+002915	3038 5	8	13.84	1.72	0.82	+	
269	ESO020-003	115514.0−784436	2733 9	8	14.33	2.05	0.56	+	
270	NGC4025	115910.2+374737	3217 7	6	12.33	2.07	0.87		F
271	6dF...	120227.5−190602	2268 74	9	13.38	1.87	0.3 :	+	
272	ESO505-025	121045.1−264215	1625 74	9	13.36	1.75	0.48	+	
273	AM1213-220	121557.8−222530	2141 5	10	14.36	1.89	0.62	+	pec
274	SDSS...	122703.0+413423	2104 5	8	14.07	1.75			
275	MCG-02-32-012	122758.8−133130	3249 37	−2	11.75	1.95	0.3 :	+	
276	NGC4529	123251.6+201101	2468 5	5	12.93	1.72	0.86		F
277	ESO442-013	123713.5−282934	1269 6	6	11.90	1.63	1.54	+	
278	UGCA291	123837.3+555533	3364 58	9	13.69	2.30		+	F,Mrk
279	SDSS...	124417.4+594308	3054 5	9	14.72	1.65		+	
280	IC3740	124530.6+204857	2602 65	4	12.81	2.16	0.7 :		
281	SBS1245+542	124809.9+540127	3437 69	8	11.96	2.30		+	IR,Mrk
282	SDSS...	125446.3+153530	2564 11	9	14.29	1.76	0.3 :		
283	MCG+09-21-092	130255.7+554140	1472 14	9	13.94	1.84	0.55		F
284	MCG+08-24-030	130321.3+481951	2595 56	5	12.83	1.70		+	
285	UGC08166	130352.5+105821	2853 5	6	12.68	1.92	0.94	+	F,KIG
286	UGC08224	130821.6+392740	3328 75	5	12.69	1.66	0.73	+	F
287	CGCG101-017	131556.3+174538	1178 37	9	14.48	1.93	0.3 :	+	KIG
288	DDO171	131841.2−082647	1150 5	8	11.38	1.83	0.70	+	
289	NGC5089	131939.3+301523	2138 11	3	10.86	1.89	0.92	+	IR
290	NGC5116	132255.6+265850	2887 5	5	9.90	2.01	0.88		IR
291	UGC08509	132818.9+673753	1162 5	9	13.89	1.94		+	
292	SDSS...	133047.8+395446	1290 5	9	15.53	1.65			
293	UGCA362	133305.9+685138	1676 75	9	13.53	1.78		+	IR,Mrk
294	UGC08578	133535.6+291301	872 10	9	13.31	2.28	0.54		Mrk
295	DDO180	133810.3−094805	1153 9	8	9.99	1.81	1.15	+	IR
296	UGC08647	133948.1+311725	776 5	10	14.08	2.18	1.01		
297	MCG-01-35-010	134537.0−055923	1333 11	8	12.90	1.75	1.66		IR

(1)	(2)	(3)	(4)		(5)	(6)	(7)	(8)	(9)	(10)
298	KK220	134736.5+331222	812	5	10	14.98	2.18	−0.08	+	
299	UGC08737	134816.7+680506	1959	5	4	9.69	1.65	0.54	+	IR,F
300	ESO577-038	134825.7−185220	1719	5	7	13.49	2.70	1.25	+	F
301	KK224	134857.3+433601	1244	5	10	14.79	1.71	0.26		
302	HIPASSJ1349-12	134910.0−124535	1246	9	8	12.99	1.81	0.83	+	pec
303	CGCG102-075	135305.4+155040	3019	41	1	11.10	2.65	0.5 :	+	
304	DDO184	135524.9+174743	939	5	8	10.89	1.81	1.25	+	pec
305	UGC08894	135747.6+632351	1938	11	8	13.82	1.73	0.86	+	
306	ESO008-004	135748.0−830449	2208	5	6	11.72	1.64	1.16	+	IR
307	MCG+10-20-057	135842.9+615146	1658	9	9	13.87	1.79		+	
308	CGCG018-021	140043.0−003020	3361	21	8	13.71	1.93	0.06	+	
309	NGC5470	140632.0+060146	962	5	4	9.96	1.75	0.96	+	IR,F
310	UGC09024	140640.6+220412	2331	5	2	13.49	1.61	0.92	+	pec
311	ESO511-008	141128.6−261214	2440	35	2	11.09	1.69	0.38	+	IR
312	NGC5510	141337.2−175902	1309	19	8	11.04	1.67	1.16	+	IR
313	NGC5523	141452.3+251903	1073	5	6	9.74	1.96	1.46	+	IR,F,KIG
314	PGC051218	141960.0−101150	3286	29	7	13.37	1.74	0.65	+	
315	UGC09193	142113.8+364434	770	5	10	14.62	2.23	0.49	+	
316	ESO446-055	142129.4−275602	2416	6	4	12.89	2.07	0.59	+	
317	DDO189	142232.2+452302	803	5	8	13.13	1.63	1.41	+	
318	HIPASSJ1424-16B	142429.0−165858	1352	9	8	12.01	1.67	1.10		
319	DDO190	142443.4+443133	263	6	10	11.00	2.49	1.39	+	
320	KKSG46	142826.6−085516	1439	9	10	14.30	1.60	0.74	+	
321	UGC09320	142958.4+365224	859	6	8	13.88	2.21	0.69	+	
322	ESO385-032	143011.9−365752	2646	5	5	9.71	1.74	1.04	+	IR
323	6dF...	143047.8−091327	2486	74	8	12.82	2.06	0.5 :		
324	SDSS...	143208.7+383122	1492	71	9	14.75	2.28			
325	LSBCD512-02	143320.1+265950	883	5	10	13.08	2.70	0.38	+	
326	KKSG47	143525.0−170947	1448	5	10	15.03	2.25	0.96	+	
327	2MASX...	143839.3−105407	3338	74	3	12.03	2.05	0.5 :	+	IR
328	MRK0475	143905.5+364822	655	30	9	13.95	2.13	−0.82	+	Mrk
329	ESO386-013	144304.3−332926	1205	9	10	12.41	2.64	0.67	+	
330	SDSS...	144310.9+382045	2875	30	6	13.40	2.10		+	
331	UGC09497	144412.8+423744	884	42	7	13.16	1.74		+	
332	UGC09519	144621.1+342214	1782	26	0	10.23	1.62		+	IR
333	SDSS...	144827.7+385233	1938	37	9	14.58	2.55			
334	MCG-01-38-003	144848.0−034259	868	9	9	12.22	1.90	1.39	+	
335	UGC09540	144852.0+344242	895	5	8	14.80	2.30	0.68	+	
336	ESO386-029	145323.3−360511	1392	74	8	12.12	2.64	0.38	+	
337	UGC09588	145411.9+301232	2939	16	9	12.47	1.96		+	IR
338	2MASX...	145739.4+263953	1477	75	9	13.63	2.30		+	pec
339	NGC5832	145745.7+714056	657	5	8	10.28	1.85	1.44	+	IR,KIG
340	ESO581-012	150004.9−223926	3350	9	7	13.79	2.19	0.92		IR,F,pec
341	UGC09676	150330.6+274929	2962	5	7	12.14	2.53			
342	UGC09730	150403.0+773804	2353	11	6	12.78	2.38	0.78	+	IR,KIG
343	PGC1067957	150704.8−034202	1638	74	9	13.36	2.05	0.48	+	
344	PGC054003	150737.3−175450	2984	5	8	14.32	1.69	1.03	+	
345	UGC09739	150855.4+254402	1441	5	7	12.56	2.30	0.73	+	KIG
346	UGC09764	151038.2+645354	2444	11	7	13.18	1.97	1.19	+	
347	ESO513-022	151200.7−240236	3469	74	4	11.71	1.77	0.92		IR,pec
348	FGC1874	151532.1+493714	2668	14	7	14.47	2.18	0.10		F
349	CGCG221-048	151701.1+394144	978	39	9	13.66	2.99			
350	CGCG106-029	151754.3+161841	766	5	10	13.22	2.88	0.11	+	
351	SDSS...	151832.1+310940	1626	61	10	14.57	2.44			
352	UGC09814	151925.1+110315	3256	5	8	12.75	2.78	0.51	+	IR
353	IC4538	152111.6−233930	2755	18	5	9.45	1.83	0.80	+	IR
354	ESO449-009	152311.9−322419	3243	74	2	10.82	2.81	0.72	+	
355	UGC09880	153044.4+471908	2730	5	8	13.83	2.40	0.69		
356	UGC09875	153047.5+230357	2072	5	8	14.18	1.95	0.68	+	
357	UGC09893	153257.3+462710	817	9	10	12.61	2.75	1.02	+	KIG
358	KKR21	153700.6+204742	1798	5	8	13.22	2.51	0.75	+	

(1)	(2)	(3)	(4)		(5)	(6)	(7)	(8)	(9)	(10)
359	6dF...	153729.3−285308	2618	74	8	12.65	1.82	0.7 :	+	
360	NGC5964	153736.3+055824	1468	5	7	11.79	1.67	1.46	+	IR,KIG
361	SDSS...	153928.7+005637	3006	22	7	13.82	2.27	0.5 :	+	
362	UGC10023	154609.7+065354	1440	5	8	12.01	1.67	0.70	+	
363	UGC10025	154624.4+025039	1538	5	8	13.90	2.26	0.71		F
364	UGC10058	155024.2+255521	2257	5	8	14.16	2.08	0.72		
365	UGC10125	155206.6+835136	1867	5	8	13.77	2.08	1.08	+	
366	UGC10119	155438.5+791025	2441	19	4	13.18	2.41			
367	HIPASSJ1558-10	155820.0−103207	906	9	8	12.06	1.84	1.07	+	
368	CGCG319-040	160227.9+642112	1813	20	6	13.16	2.42			IR
369	UGC10175	160437.7+304253	952	6	8	12.46	2.48	0.66		
370	2MASX...	160511.0+462331	3155	74	5	13.57	2.50		+	
371	KKSG48	160540.9−043419	1616	5	10	12.64	1.60	0.86	+	
372	2MASX...	160705.2−112552	1786	74	4	11.43	2.59	0.5 :	+	
373	UGC10247	160926.0+600517	3210	5	8	12.77	1.71	0.76	+	
374	MCG-01-41-006	160936.8−043713	847	9	10	11.92	2.38	0.84		
375	SHOC 529	161111.5+482004	3011	16	9	13.15	2.20			
376	UGC10281	161320.6+171134	1182	5	10	15.39	3.00	0.67	+	
377	HIPASSJ1615-17	161545.3−175030	2330	9	8	11.96	3.32	0.90	+	
378	DDO204	161618.3+470247	908	6	8	11.03	2.61	1.17	+	IR
379	KKR26	161644.6+160509	2347	5	10	14.56	1.79	0.36		
380	MCG-02-41-001	161715.8−114355	960	5	3	9.80	1.84	1.60	+	IR
381	2MASX...	162047.4+470354	3218	35	9	14.05	2.34		+	
382	LSBCD584-05	162123.8+205156	3220	5	8	14.01	1.76	1.27		
383	UGC10383	162442.8+643044	2990	5	8	12.31	2.30	0.82	+	
384	UGC10419	163006.1+274158	2762	5	8	14.34	2.38	0.62		
385	UGC10437	163107.6+432055	2795	13	6	12.71	3.08	1.10		KIG
386	SDSS...	163424.7+245741	1131	40	9	15.51	1.85		+	
387	UGCA412	163521.1+521253	2865	33	9	13.05	2.39	−0.35	+	IR,Mrk
388	PGC165693	164302.7−204009	1174	5	7	10.33	2.80	0.47	+	IR
389	2MASX...	164819.4−103139	1595	9	8	11.54	2.56	1.07	+	
390	UGC10589	165025.0+555027	2351	11	6	12.25	3.00		+	
391	DDO206	165421.5+530647	1317	5	8	12.59	1.88	0.95	+	IR
392	KKR30	165638.5+075955	1584	6	8	13.87	2.01	0.67	+	
393	NGC6283	165926.6+495519	1317	36	4	10.83	1.88		+	IR
394	HIPASSJ1700-12	170006.3−120001	1327	9	8	13.46	3.07	0.76		
395	UGC10721	170825.6+253103	3091	5	4	10.57	2.12	0.72	+	
396	KKR34	171242.1+135428	1640	5	10	14.78	1.93	0.61	+	
397	NGC6339	171706.5+405042	2326	6	6	10.96	1.89	1.05		IR
398	DDO207	171951.0+142401	1698	5	9	12.61	1.88	0.64	+	KIG
399	CGCG226-010	172410.3+432711	2382	38	5	12.65	1.92			IR
400	UGC10854	172446.4+581221	3052	11	6	12.30	2.01	0.49		
401	UGC10899	173335.8+204604	3402	5	4	11.92	1.85	0.76	+	
402	UGC10901	173354.1+052834	2956	8	6	13.62	2.91	0.96	+	
403	KUG1736+636	173637.1+633502	1454	75	9	13.00	2.51		+	IR
404	IC1265	173639.4+420518	2397	6	2	10.99	1.92	0.64		IR
405	NGC6434	173648.8+720520	2741	6	4	9.96	2.07	1.00	+	IR
406	6dF...	173924.3−674906	3075	9	6	12.72	1.64	0.68	+	
407	VII Zw 744	174137.7+830759	2120	69	−1	12.02	2.37		+	KIG
408	HIPASSJ1745-59	174526.7−593128	3113	9	8	13.34	1.93	0.63	+	
409	KKR36	174616.3+020658	3107	6	9	13.59	2.45	0.59	+	
410	UGC10985	174804.4+144429	1969	5	8	10.71	2.11	0.68		IR,F
411	MRK1119	175236.9+374453	3431	36	0	12.04	2.47		+	IR,Mrk
412	NGC6542	175938.6+612134	932	35	2	11.03	2.08	0.32	+	IR,F
413	UGC11109	180414.0+464414	1820	5	10	14.46	2.75	0.72		
414	UGC11220	182325.5+405643	1706	5	10	14.45	2.78	0.98	+	
415	UGC11231	182538.3+292232	3135	75	6	13.38	2.00	0.27	+	F
416	UGC11295	183307.5+752401	2632	5	6	13.58	2.08	1.04	+	F
417	NGC6689	183450.3+703126	758	5	6	10.11	1.72	1.45	+	IR,KIG
418	UGC11382	185357.7+743936	2679	6	10	13.60	2.08	0.19	+	
419	UGC11400	190025.5+790220	1991	5	8	14.04	2.54	0.33		

(1)	(2)	(3)	(4)		(5)	(6)	(7)	(8)	(9)	(10)
420	NGC6762	190537.1+635603	3205	28	0	10.19	2.18		+	
421	IC4819	190707.3−592801	1728	10	6	11.01	1.65	1.45	+	F
422	NGC6789	191641.1+635824	136	11	9	12.22	1.65	0.0 :	+	
423	NGC6796	192131.1+610855	2477	14	4	9.56	2.32	1.38	+	IR,F
424	ESO525-005	192645.2−272514	1995	9	10	13.77	2.14	0.41		
425	HIPASSJ1926-74	192727.1−740458	2444	9	9	14.51	2.23	0.36		
426	2MASX...	193159.0−362646	2769	11	5	12.99	2.31	0.11		
427	ESO594-011	194042.4−221614	1874	5	5	11.97	2.46	0.23	+	
428	UGCA416	194822.0−180442	1864	19	8	12.34	1.93	1.02	+	
429	2MASX...	195015.9−101724	2163	10	4	11.63	1.86	1.06	+	
430	UGC11496	195302.0+673954	2402	7	8	13.19	1.72	0.80	+	
431	KK246	200357.4−314054	436	49	10	13.56	3.22	0.92	+	
432	IC4968	201450.2−644754	3348	74	5	11.60	1.66	0.5 :		
433	IC4986	201711.6−550211	2080	16	7	11.94	2.02	1.30		
434	FGC2266	201729.1−105051	2010	5	6	12.72	3.20	0.99	+	F
435	2MASX...	201731.5+720726	2692	22	−1	10.71	1.95		+	IR
436	6dF...	202031.8−045358	1567	9	8	13.66	2.15	1.06	+	
437	UGC11565	202802.9+045743	3318	9	6	11.71	2.68	1.03	+	IR,F
438	UGC11566	202811.9+001718	1875	35	4	10.91	1.79	0.3 :	+	IR,Mrk
439	AM2024-612	202843.2−611819	3377	74	8	13.44	1.72	0.50		
440	KKR54	203558.8−011859	1929	7	10	14.23	1.79	0.3 :	+	
441	2MASX...	203857.3−634616	1536	9	9	13.60	1.94	0.57	+	
442	IC5028	204322.0−653852	1498	9	10	12.78	1.94	0.92		
443	IC5052	205201.6−691136	447	7	7	8.87	2.65	2.20	+	IR
444	ESO598-017	210230.8−192752	2546	74	8	13.13	2.83	0.41	+	
445	ESO341-032	210333.4−392647	2762	9	9	11.53	1.64	0.98	+	IR
446	ESO464-023	210656.0−300542	2619	75	8	14.29	2.20	0.3 :		
447	ESO187-051	210733.1−545702	1313	32	8	12.54	2.10	1.09		pec
448	MCG-01-54-003	211005.1−034206	2425	5	5	10.94	2.26	0.56	+	
449	ESO107-016	211606.2−644901	1704	48	7	12.30	1.88	1.46	+	F
450	CGCG471-002	211652.9+241215	3164	29	0	10.41	2.29	0.5 :	+	IR
451	MCG-01-54-016	212559.8−034836	3127	5	7	13.26	2.08	0.86		F
452	ESO530-051	212744.0−234006	1904	43	8	12.89	2.31	0.54	+	
453	NGC7077	212959.6+022451	1369	5	9	11.36	2.83	0.34	+	IR,Mrk
454	ESO465-009	213515.1−305041	3195	59	5	12.32	1.66	0.41		
455	2MASX...	213554.0−030853	3073	5	4	11.16	2.08	0.45		IR
456	UGC11782	213809.7+085741	1359	5	8	11.71	2.37	1.05	+	
457	6dF...	214226.9−061954	1448	74	9	13.36	1.96	0.64		
458	CGCG402-023	215102.8+061436	1698	28	9	12.77	2.60	0.16	+	KIG
459	ESO532-002	215322.1−263441	1858	5	10	15.98	1.98	0.64	+	
460	UGC11908	220635.2+160319	2039	5	9	13.84	1.89	0.58	+	
461	UGC11921	220915.6+142136	1939	5	8	13.34	1.86	1.18	+	KIG
462	ESO404-037	221035.2−365031	2610	5	8	14.19	1.88	1.34	+	
463	APMBGC...	221848.9−461303	1185	45	9	13.96	1.65			
464	IC5201	222057.4−460209	893	5	6	10.16	1.65	1.97	+	IR
465	ESO238-005	222230.1−482418	671	9	10	13.19	1.99	1.18	+	
466	DUKST405-048	222310.0−333953	2512	74	9	13.94	1.65	0.3 :	+	
467	UGC12010	222318.7+053202	3037	5	5	11.37	2.56	0.70	+	F
468	ESO289-026	222333.2−421628	2421	5	8	11.93	1.85	1.35		IR
469	ESO190-011	222703.3−521536	2788	9	8	12.26	1.89	0.58	+	
470	ESO345-021	223237.8−380254	3193	49	4	12.20	2.15	0.5 :		
471	ESO238-018	223543.8−505326	2848	75	5	12.39	1.89	0.70	+	IR
472	DDO214	223635.0−025424	1887	5	8	10.56	1.93	1.08	+	
473	NGC7328	223729.3+103154	3054	21	5	9.60	1.75	1.05	+	IR,KIG
474	UGC12141	223814.8+804038	2353	5	7	11.80	1.62	0.92	+	F,KIG
475	UGC12151	224133.9+002404	1966	5	8	11.27	1.79	1.20	+	
476	SDSS...	224359.9−100701	1115	6	10	15.03	2.78	0.3 :	+	
477	PGC133414	224431.4−281547	2604	21	9	13.68	1.98	0.5 :		
478	UGC12178	224508.7+062551	2160	5	8	10.52	1.83	1.37	+	IR,KIG
479	HIPASSJ2250+00	225024.2+005247	1902	9	10	14.43	1.79	0.5 :	+	
480	UGC12221	225025.6+825237	2314	11	7	11.07	1.62	1.14	+	IR,KIG

(1)	(2)	(3)	(4)	(5)	(6)	(7)	(8)	(9)	(10)
481	UGC12213	225103.0+071745	3438	5	7	12.47	1.73	0.92	+	
482	NGC7406	225356.2−063445	1786	8	4	10.41	2.21	0.41	
483	MCG-05-54-004	225445.2−265325	868	37	9	13.31	2.17	1.01		IR
484	ESO469-006	225508.0−305520	3027	53	−1	11.41	2.05	0.5 :		IR
485	LSBCF469-02	225721.5+275852	3233	6	8	15.67	2.93	0.42	+	
486	ESO603-031	225726.4−175308	2391	10	2	12.22	2.31	0.20	+	
487	PGC938611	225946.2−132322	1361	9	9	12.57	2.41	0.37		
488	NGC7460	230142.9+021549	3401	18	5	9.95	1.77	0.07	+	IR
489	PGC132632	230313.0−352415	2157	43	6	13.94	1.63	0.48	+	
490	PGC141060	230341.3+234108	1432	6	10	14.13	2.67	0.50		
491	UGC12340	230433.9+270921	1340	8	8	12.63	2.67	0.87	+	
492	ESO604-004	230628.9−174710	3120	5	8	13.72	2.56	0.94	+	
493	HIPASSJ2307-61	230720.8−614052	3108	9	10	15.06	1.74	0.41	+	
494	2MASX...	231122.0−231525	3490	74	3	13.00	2.77	0.7 :		
495	MCG-03-59-001	231136.7−152835	2201	20	7	12.12	1.72	0.93	+	F
496	ESO407-014	231739.5−344727	2782	7	5	10.80	2.15	1.03	+	IR
497	6dF...	231803.9−485936	2275	74	9	14.30	1.67	0.3 :	+	
498	UGC12495	231848.5+163738	2869	21	6	13.71	1.87	0.66	+	
499	KUG2316+162	231921.9+163401	3187	18	5	13.34	1.86	−0.07	+	
500	KKR75	232011.2+103723	1703	5	10	15.44	1.62	0.54	+	
501	FGC2498	232442.0−024730	2726	13	7	13.76	1.96	0.3 :	+	F
502	IC5321	232620.0−175723	2984	11	5	12.29	2.29	1.01	+	IR
503	UGC12070	233157.3+780903	1724	5	10	13.24	2.10	0.96	+	
504	ESO347-029	233627.2−384657	1553	8	8	11.28	1.74	1.46	+	
505	UGCA441	233739.6+300746	1660	7	9	12.06	2.89	−0.14	+	IR,Mrk,KIG
506	UGC12713	233814.7+304233	568	8	9	13.60	2.09	0.88	+	
507	UGC12729	234020.8+011445	2074	55	4	12.24	2.21	0.98	+	KIG
508	2MASX...	234056.8−190507	1637	30	9	12.35	2.12	0.34		IR
509	ESO292-014	234235.2−445417	1500	55	6	10.75	1.68	1.06	+	IR,F
510	PGC072271	234425.9−164849	1680	9	10	13.36	2.12	0.73	+	
511	HIPASSJ2344-07	234429.5−073545	1983	9	8	13.25	2.52	0.76		
512	UGC12771	234532.7+171512	1535	5	10	13.90	3.25	0.46	+	
513	ESO149-001	234749.9−570415	1800	11	8	9.49	1.87	1.82	+	IR
514	PGC812517	234951.8−223256	1098	9	9	13.69	2.88	0.46	+	
515	NGC7764	235054.0−404342	1691	69	8	10.30	1.74	1.05	+	
516	ESO149-003	235202.8−523440	501	9	8	12.41	2.48	1.15	+	
517	UGC12856	235645.3+164850	2017	8	8	13.21	1.67	1.39	+	pec
518	UGC12857	235647.6+012118	2642	7	5	11.26	1.75	1.36	+	IR,F,KIG
519	ESO028-007	235801.0−732711	2374	9	7	13.00	3.46	0.86		
520	NGC7800	235936.7+144826	1976	6	10	11.26	1.61	1.71	+	IR,pec

The least frequent among the isolated galaxies are the lenticular and Sa–Sb galaxies ($T = 0 - 3$). In the KIG and 2MIG catalogs of isolated galaxies the median of the distribution by type lies between $T = 3$ (Sb) and $T = 4$ (Sbc), i.e. a half of the population of these samples has well-defined bulges. The relative number of irregular galaxies in the KIG and 2MIG catalogs is less than 4%.

However, a considerable part of differences in the morphological composition of the LOG, KIG and 2MIG catalogs is due to the selection effects. As a distance-limited sample, the LOG catalog contains much more galaxies of low luminosity ($T = 10, 9$) than the KIG and 2MIG catalogs, where the selection of galaxies was based on their apparent magnitude, i.e. luminosity. We observe a similar effect on the example of galaxies in the Local Volume with $D < 10$ Mpc, where about 70% of the total sample belong to the types 9 and 10, i.e. to irregular galaxies. We also note that among

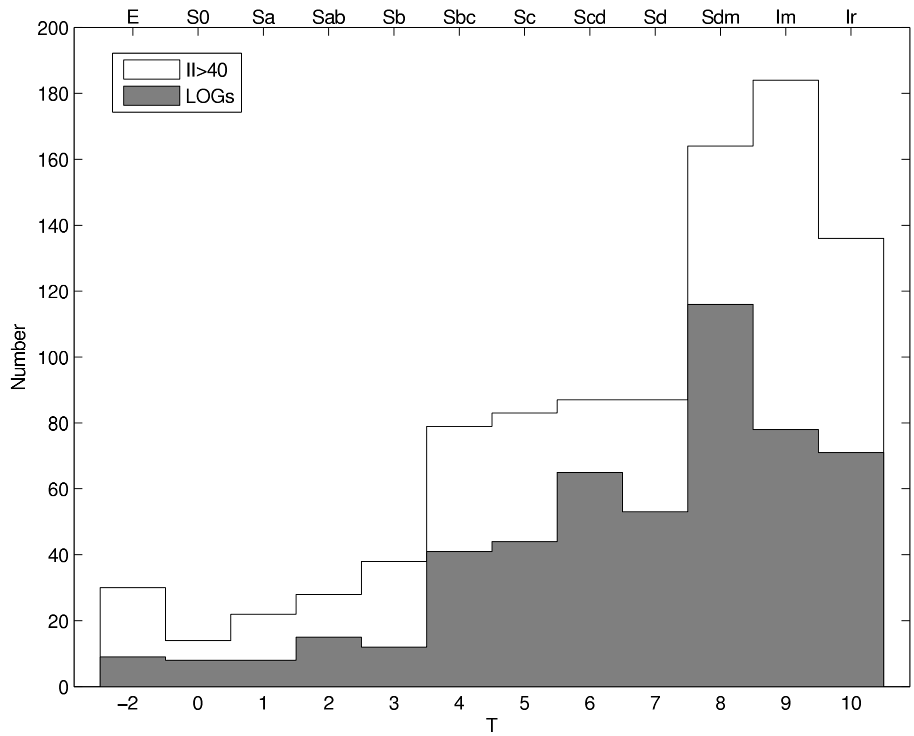

Figure 4. The distribution of isolated galaxies by morphological type. The upper histogram shows all the 990 galaxies with $II > 40$, the gray histogram—520 galaxies from the LOG catalog.

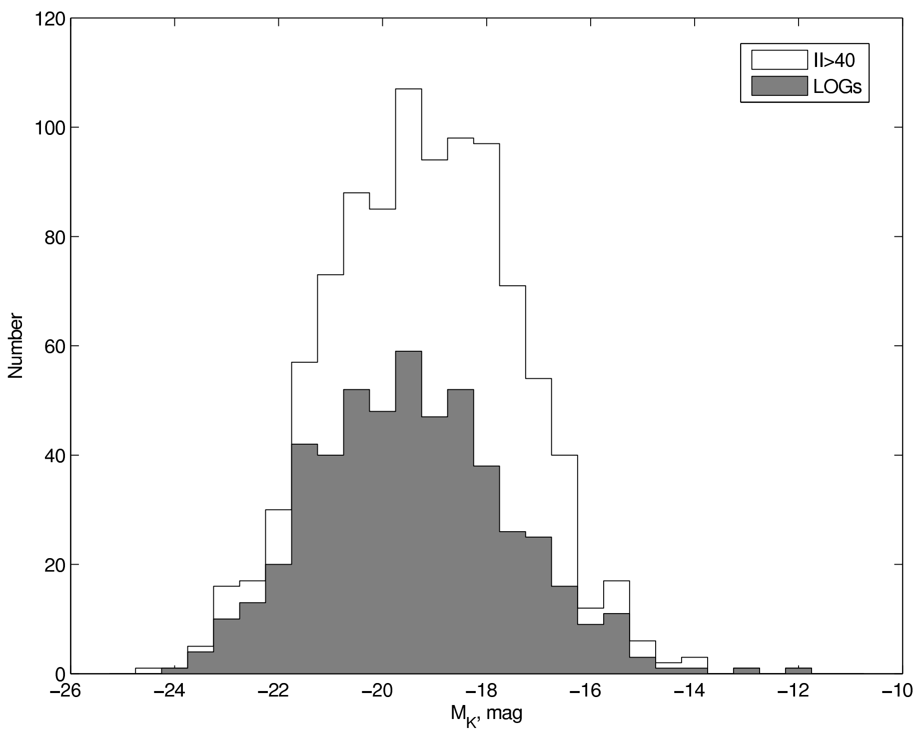

Figure 5. Luminosity function of isolated galaxies. Gray marks the catalog distribution of the LOG galaxies.

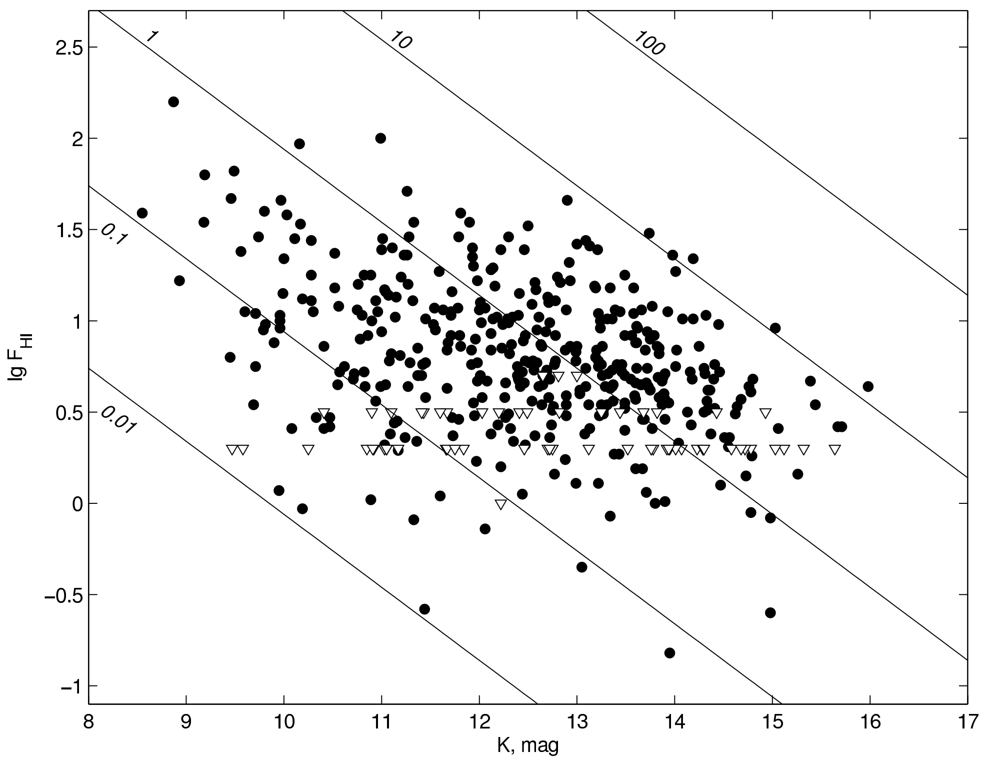

Figure 6. The apparent K magnitudes and the HI flux logarithm for the LOG galaxies. The triangles show the upper values of the HI flux. The sloping lines correspond to the constant ratio M_{HI}/L_K, equal to 0.01, 0.1, 1, 10 and 100 in solar units.

33 isolated galaxies, common to the KIG and LOG catalogs, the peak of the distributions by the morphological type falls on $T = 6$ (Scd), i.e. on the spirals without apparent bulges.

It must be emphasized that it is usually difficult to find the evolutionary reasons for the differences of two samples by morphological composition, since these differences are masked by the selection effects of the sample itself. For example, two catalog samples of isolated galaxies, KIG and 2MIG, show an apparent difference in the relative number of galaxies with bulges. However, this is an expected difference, and it is due to the fact that the galaxies in the 2MIG catalog were selected by luminosity in the near infrared, where the galaxy bulges are more prominent than in the optical B-band.

As follows from the last column of Table 1, about 30% of the LOG galaxies are the infrared IRAS-sources. Their distribution by morphological type varies considerably from the total distribution (see Fig. 4 in [14]). The maximum of the distribution of isolated IRAS galaxies falls on the $T = 4-6$ types. Such a difference with the total sample has a highly selective character, since the IRAS fluxes are closely correlated with the mass of the dust component of galaxies, which is most pronounced

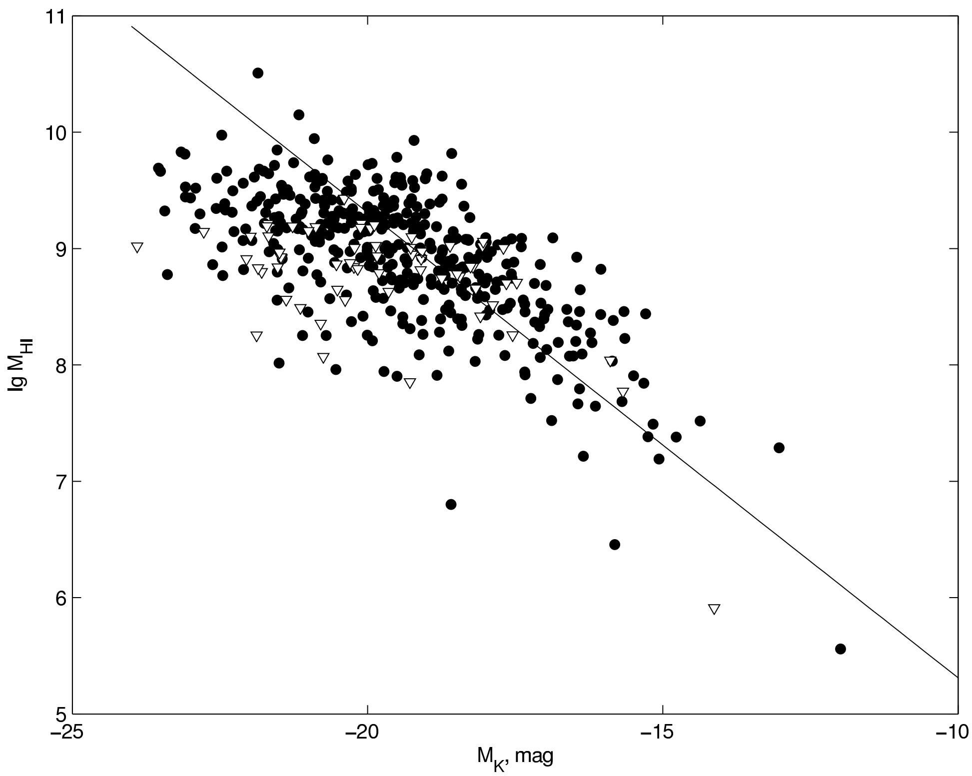

Figure 7. The logarithm of the hydrogen mass vs. the absolute K magnitude in LOG galaxies. The solid line corresponds to the case $M_{gas} = M_{stars}$ in the galaxy.

namely in the Sc galaxies.

Current models of galaxy formation imply that the E and S0 galaxies are formed by multiple mergers of disk-shaped and irregular galaxies. Clusters usually involve a permanent mechanism of transformation of spiral galaxies into lenticular by sweeping out the gas, hence preventing further star formation. Thus, it is expected that the E and S0 galaxies should occur mainly in the regions of high matter density. Indeed, the KIG and 2MIG catalogs contain only 16% and 18% of the E + S0 galaxies, respectively, which is lower than their average cosmic abundance (about 24%).

There are only 17 galaxies in the LOG catalog that we classified as E and S0 (T<1). A list of these galaxies, making up less than 4% of our sample is presented in Table 2. Hereinafter the distances to the galaxies were determined from their radial velocity V_{LG} at the Hubble constant $H_0 = 73$ km/s Mpc^{-1}.

It is noteworthy that the isolated E and S0 galaxies in the LOG differ significantly from the other E and S0 galaxies by a number of features. The isolated early-type galaxies have a rather low luminosity, their median absolute magnitude is $M_K = -21.7$ or $M_B = -17.7$. More than a half of E and S0 galaxies in the LOG are the IRAS sources, which indicates the presence of a

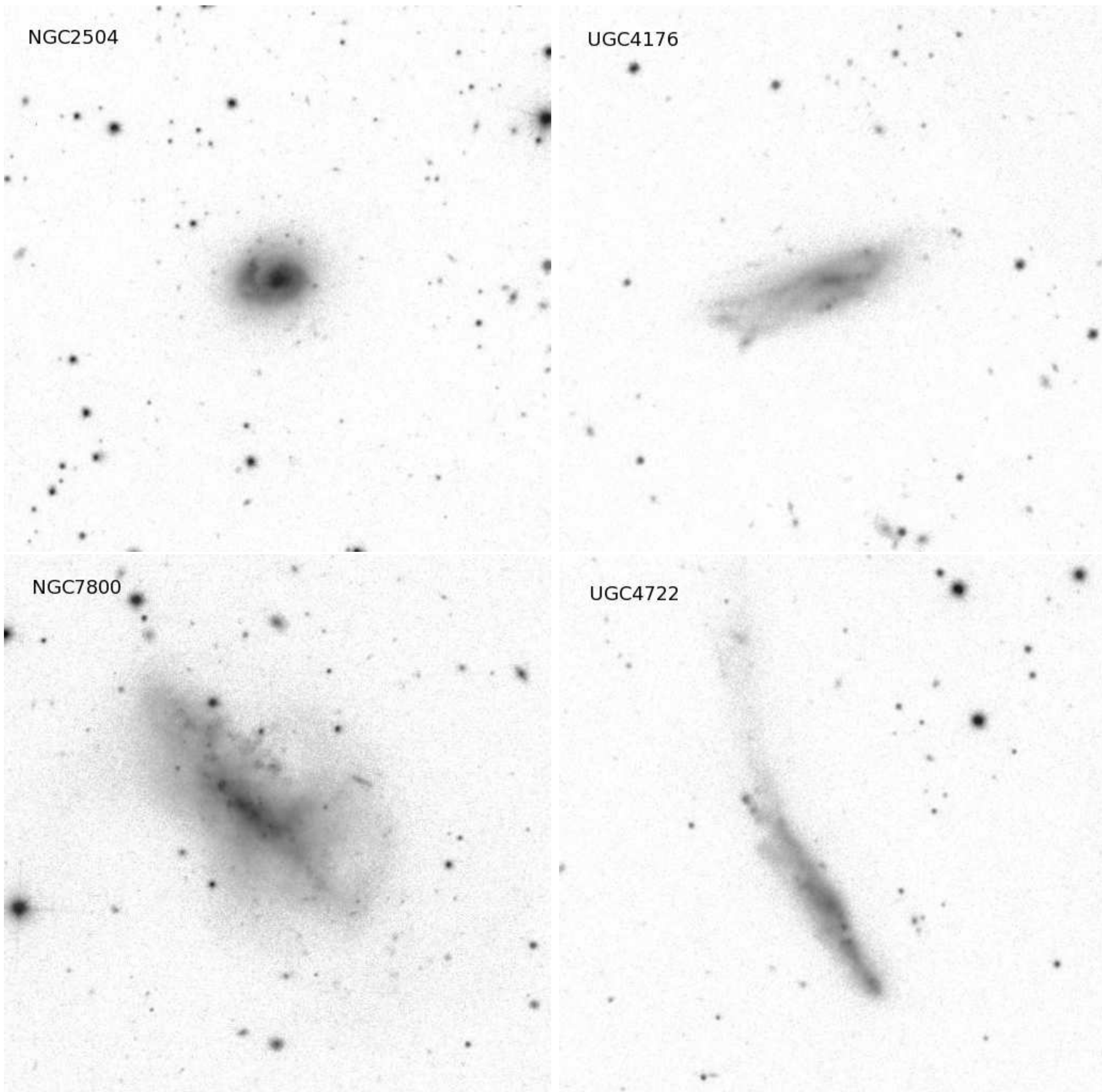

Figure 8. Examples of isolated galaxies with peculiar structures: NGC 2504, UGC 4176, NGC 7800, and UGC 4722.

considerable amount of dust. Some of them (NGC 404, UGC 1198, UGC 5467) reveal the HI line fluxes, corresponding to the masses of neutral hydrogen of the order of $10^8 - 10^9 M_\odot$. We can assume that during their evolution the isolated E and S0 galaxies undergo a significant impact (inflow) of the intergalactic medium, where about 80% of the universe's baryons are concentrated [15].

Figure 5 demonstrates the distribution of all types of isolated galaxies by absolute K magnitudes. The galaxies that are included in the LOG catalog (in gray) have approximately the same luminosity function as all the 990 galaxies satisfying the condition $II > 40$. In other words, an additional rejection of isolated galaxies using Karachentseva's criterion does not introduce any significant selection by luminosity.

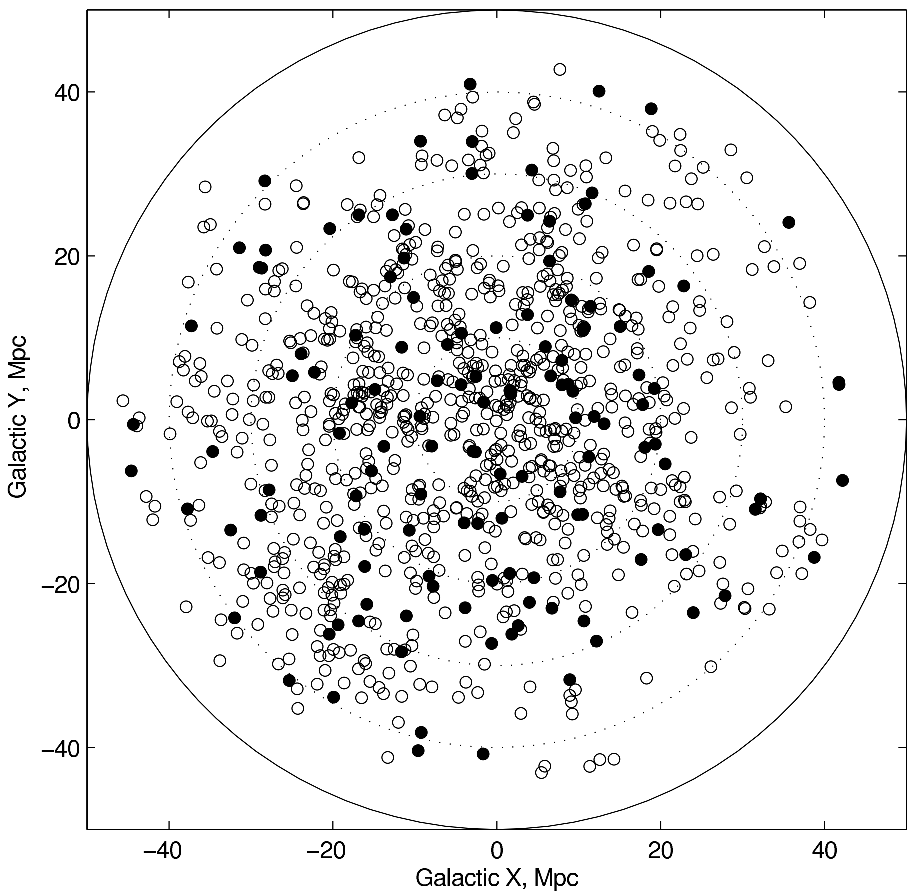

Figure 9. The distribution of 520 LOG galaxies in Cartesian Galactic coordinates. Galaxies with developed bulges (T< 4) are shown by solid circles.

Table 2. Galaxies of early morphological types (T < 1) in the LOG catalog

LOG	V_{LG}	T	M_K	lg M_{HI}	Note
31	3066	0	−21.5	<8.9	IRAS
50	218	−3	−18.9	7.9	IRAS
62	1408	−2	−20.6	8.0	IRAS
104	3449	−1	−23.9	<9.0	IRAS
169	2796	0	−22.1	–	
220	3043	0	−22.1	<8.9	
231	2768	−2	−22.1	9.2	IRAS
256	1876	0	−19.0	–	
264	2226	−3	−21.6	<8.8	
275	3249	−2	−21.5	<9.0	
332	1782	0	−21.7	–	IRAS
407	2120	−1	−20.3	–	
411	3431	0	−21.4	–	IRAS
420	3205	0	−23.1	–	
435	2692	−1	−22.2	–	IRAS
450	3164	0	−22.8	<9.1	IRAS
484	3027	−1	−21.7	<9.1	IRAS
Median			−21.7	<8.9	

Table 3. Nearby isolated galaxies with peculiar structures

LOG	V_{LG}	T	M_K	Structural features
12	1636	2	–19.6	a weak external ring
58	677	10	–16.2	dIr + cirrus?
100	2777	8	–19.2	a wide curved tail
114	2327	8	–19.8	flocky
163	964	10	–16.9	flocky
179	2419	4	–21.2	tail or arm from a compact body
180	3092	7	–20.5	asymmetrical
197	1705	7	–19.2	a wide tail
219	1811	9	–18.7	knotted with a tail
243	2377	8	–19.5	knotted
260	2635	10	–20.3	knotted
273	2141	10	–18.0	knotted
302	1246	8	–18.2	hammer-like
304	939	8	–19.4	faint blue knots in the outskirts
310	2331	2	–19.0	a weak extended periphery as in Malin-1
338	1477	9	–17.9	comet-like
340	3350	7	–19.5	asymmetrical
347	3469	4	–21.7	a distorted tail
447	1313	8	–18.7	asymmetrical, flocky
517	2017	8	–19.0	distorted, flocky
520	1976	10	–20.9	disturbed, with loops
Median		8	–19.2	

Figure 6 presents the distribution of LOG galaxies by apparent K magnitudes and by the logarithms of the integrated HI line flux. Each galaxy with measured HI flux is marked by a circle, and the galaxies with an estimate of the upper limit of HI flux are marked by triangles. Apart from them, about 12% of galaxies in this catalog have not yet been observed in the HI line. The diagonal lines in the figure correspond to the values of the hydrogen mass-to-stellar mass ratio, equal to 0.01, 0.1, 1, 10 and 100. Here the mass ratio was defined as

$$\log(M_{HI}/M_*) = \log F_{HI} + 0.4m_K - 5.94$$

at the absolute K-luminosity of the Sun $M_K(\odot) = 3.28^m$. These data show that in almost all the galaxies the M_{HI}/M_* ratio lies within the range from 0.01 to 10 with a median value of 0.7. Taking into account the correction for helium and molecular hydrogen (the factor of 1.85 according to [15]), the characteristic ratio of the mass of gas and stars in the considered galaxies is equal to 1.3. Hence, a typical isolated LOG galaxy has transformed into stars less than a half of its gas reserves. And in some isolated galaxies (UGC 3672) more than 90% of baryons still reside in the form of the gas component.

It is well known that the mass ratio of gas to stars shows a tendency of increase from normal to dwarf galaxies. This could mean that the phase of active star formation in dwarf galaxies comes later than normal, or that the star formation in dwarf systems advances in a more slow rate. Figure 7 reproduces the relationship between the logarithm of hydrogen mass and the absolute K magnitude of isolated galaxies. The objects with an estimate of the upper limit of HI flux are marked by triangles. The straight line in the figure fixes the value of $M_{HI} = M_*$. The galaxies with higher luminosity ($M_K < -19.5^m$) show a significant hydrogen mass deficiency with respect to this line.

5. PECULIAR ISOLATED GALAXIES

The standard cosmological ΛCDM model predicts the existence of a large number of massive invisible bodies (dark sub-haloes), in which the star formation process has not yet been triggered [16]. It is assumed that such dark clumps with masses on the order of $(10^6 - 10^9)M_\odot$ can be ten times more numerous than normal galaxies. The search for such objects in the HIPASS and ALFALFA surveys via the HI line emission were so far unsuccessful [17, 18].

The presence of a numerous population of dark massive objects among the galaxies should give a large number of tight interactions "galaxy–dark body." The expected result of their close approach could be a distortion of the structure of a normal (bright) galaxy, or a "visualization" of a dark component via an inflow of matter from the ordinary galaxy. It is obvious that the cases of "unmotivated" interaction with an invisible object are to be searched just among the isolated galaxies. Karachentsev et al. [19, 20] have found 8 examples of isolated galaxies from the KIG sample with pronounced structural distortions. Peculiar shapes that some of them have may be due to an asymmetric starburst or a recent merger of two galaxies. However, two galaxies: UGC 4722 and ESO 545–05 proved to match quite adequately the assumption about their interaction with a massive invisible object. The interaction effects are most pronounced in the cases where the objects of approximately the same mass approach each other. Since it is expected that the number of dark bodies increases with the decreasing mass, the search for traces of interaction with such bodies looks more promising among the most low-mass isolated galaxies.

A typical galaxy in the LOG catalog has on the average an order of magnitude lower luminosity (mass) than a typical representative of the KIG catalog. The last column of Table 1 lists 21 galaxies with a peculiar morphology. All of them are enumerated in Table 3. The reproductions of four interacting isolated galaxies from the SDSS and DSS surveys are demonstrated in Fig. 8. The existence of a very asymmetric shape (NGC 2504), a distorted spiral structure (NGC 4176), a perturbed disk with loops (NGC 7800), a broad tidal tail (UGC 4722) is rather difficult to explain without invoking the idea of interaction with an invisible massive body. However, it should be emphasized that the reported cases of peculiar structures make up only 4% of the total number of galaxies in the LOG catalog. This fact can become a strong restriction on the size of the population of dark objects with masses of about $10^8 - 10^9 M_\odot$.

6. DISCUSSION AND CONCLUSIONS

The above data show that the list of most isolated galaxies is dominated by the objects of late morphological types and low luminosity, most of which possess significant reserves of gas for the further star formation. These properties seem to be quite anticipated in the framework of the standard cosmological model. As Makarov and Karachentsev have noted [21], about 46% of galaxies are located outside the virial regions of groups and clusters, however only 18% of the total stellar mass (i.e. the luminosity of galaxies in the K-band) is located outside the groups and clusters.

All the 22 LOG catalog galaxies, located in the Local Volume of the 10 Mpc radius have a negative value of the tidal index (3). One of the closest and most isolated LOG galaxies in the Local Volume is a well-known irregular galaxy KK 246, located on the outskirts of the Local cosmic Void. The median value of the tidal index for these 22 galaxies, $TI = -1.7$, shows that the typical local density around the LOG galaxies is approximately 50 times lower than the average density in the Local Volume. This fact emphasizes the physical basis for the isolation criteria used in our catalog.

The number of galaxies in the LOG, common with the KIG catalog amounts to mere 33. A small fraction of the overlap between the LOG and KIG catalogs is due primarily to the difference in spatial volumes of these samples, which overlap by about 1/8. A detailed comparison of galaxy properties in both catalogs deserves special consideration.

What stands out is a relatively high number of "flat" spiral galaxies, seen edge-on ($N_F = 71$ in the last column of Table 1). Taken a random orientation of axes in thin spiral galaxies, their expected number in the LOG catalog should be about 18–32. The observed excess of the N_F number indicates that the thin disks with an axis ratio $a/b > 7$ can persist mainly in the sites of low matter density, where the tidal perturbations of neighbors do not cause the "warming-up" and thickening of the disc along the axis of rotation.

Quite a large number of galaxies in the LOG are the IRAS sources ($N_{IRAS} = 142$). Their distribution by morphological types is characterized by a broad maximum at the Sbc–Scd types ($T = 4 - 6$), what indicates the presence of a developed dust component in the disks of isolated galaxies. The total number of "active" galaxies (Mrk) in the LOG catalog is relatively small (18), most of them being intergalactic HII regions [22], rather than objects with active (Seyfert) cores.

Figure 9 demonstrates the distribution of 520 LOG galaxies in Cartesian Galactic coordinates in the projection on the plane of the Milky Way. The choice of such a projection reduces the effect of absorption of light in our Galaxy. In the first approximation, the distribution of isolated galaxies looks quite homogeneous, with some decrease in the number density of galaxies from the center to the periphery of the volume due to the loss of a part of dwarf galaxies at large distances from the observer. The galaxies with bulges ($T < 4$), marked by filled circles, do not reveal any increased crowding in groups compared with the later types (empty circles). The fact that the isolated galaxies avoid the volumes occupied by nearby clusters and groups, as well as nearby cosmic voids (the Local Void in the Aquila-Hercules, in the Eridanus and in the Leo) has some influence on their spatial distribution [23].

At the same time, one can recognize a slightly pronounced mutual association of the LOG galaxies with radial velocity differences of less than 50 km/s on a scale of around 0.5 Mpc. Examples of such associations are LOG 254+255, LOG 360+362, LOG 3+20+30. The presence of such non-virialized structures may indicate the existence in the regions of low density of some low-contrast filamentary structures (similar to the nearby chain in Sculptor [24]) or an association of dwarf galaxies, noted recently in [25] and [3]. The features of galaxy distribution in the regions of extremely low matter density contain important information on the formation and evolution of the large-scale structure of the universe. However, this sector of observational cosmology is still almost unexplored.

ACKNOWLEDGMENTS

This study was made owing to the support of the following grants: the grants of the Russian Foundation for Basic Research (RFBR) nos. 09–02–90414-UKR-f-a, 08–02–00627-a, and the grant of the Ministry of Education and Science of the Ukraine no. F28.2/059. The paper made use of the HyperLEDA (`http://leda.univ-lyon1.fr`) and NED (`http://nedwww.ipac.caltech.edu`) data- bases.

---

1. R.B. Tully, Astrophys. J. **321**, 280 (1987)
2. A.C. Crook, J.P. Huchra, N. Martimbeau, et al., Astrophys. J. **655**, 790 (2007).
3. D.I. Makarov and I.D. Karachentsev, Monthly Notices Roy. Astronom. Soc. (2011) (accepted).
4. V.E. Karachentseva, Soobscheniya SAO **8**, 3 (1973).

5. V.E. Karachentseva, S.N. Mitronova, O.V. Melnyk, and I.D. Karachentsev, Astrophysical Bulletin **65**, 1 (2010).
6. T.H. Jarrett, T. Chester, R. Cutri, et al., Astronom. J. **119**, 2498 (2000).
7. I.D. Karachentsev, V.E. Karachentseva, W.K. Huchtmeier, and D.I. Makarov, Astronom. J. **127**, 2031 (2004).
8. G. Paturel, C. Petit, Ph. Prugniel, et al. Astronom. and Astrophys. **412**, 45 (2003).
9. T. Jarrett, R. Chester, R. Cutri, et al, Astronom. J. **125**, 525 (2003).
10. I.D. Karachentsev and A.M. Kut'kin, Astron. Lett. **31**, 299 (2005).
11. O.V. Melnyk, V.E. Karachentseva, I.D. Karachentsev, et al., Astrofizica **52**, 184 (2009).
12. G. de Vaucouleurs, A. de Vaucouleurs, H.G. Corwin, et al., Third Reference Catalogue of Bright Galaxies, series I-III, Springer-Verlag Berlin Heidelberg New York, (1991).
13. S.S. Alam, D.L. Tucker, B.C. Lee, and J.A. Smith, Astronom. J. **129**, 2062 (2005).
14. I.D. Karachentsev, D.I. Makarov, V.E. Karachentseva, and O.V. Melnyk, ASP Conference ser. **421**, 69 (2010).
15. M. Fukugita and P.J.E. Peebles,Astrophys. J. **616**, 643 (2004).
16. A.A. Klypin, A.V. Kravtsov, and O. Valenzuela, Astrophys. J. **522**, 82 (1999).
17. J.I. Davies, Proceedings IAU Symp. №244, 7 (2008)
18. M.P. Haynes, Proceedings IAU Symp. №244, 83 (2008).
19. I.D. Karachentsev, A.E. Dolphin, R.B. Tully, et al., Astronom. J. **131**, 1361 (2006).
20. I.D. Karachentsev, V.E. Karachentseva, W.K. Huchtmeier, et al., Proceedings IAU Symp. №244, 235 (2008).
21. D.I. Makarov and I.D. Karachentsev, Astrophysical Bulletin **64**, 24 (2009).
22. L. Searle and W.L.W. Sargent, Astrophys. J. **173**, 25 (1972)
23. A.V. Tikhonov and I.D. Karachentsev, Astrophys. J. **653**, 969 (2006).
24. I.D. Karachentsev, E.K. Grebel, M.E. Sharina, et al., Astronom. and Astrophys. **404**, 93 (2003).
25. R.B. Tully, L. Rizzi, A.E. Dolphin, et al., Astronom. J. **132**, 729 (2006).